Title

Multiphysics processes in partially saturated fracture rock: Experiments and models from Yucca Mountain

Author
Rutqvist, J.

Publication Date
2012-10-20

Peer reviewed

Multiphysics processes in partially saturated fracture rock: experiments and models from Yucca Mountain

Jonny Rutqvist and Chin-Fu Tsang
Earth Sciences Division
Lawrence Berkeley National Laboratory
Berkeley, CA 947 20

July 10, 2012

Keywords: Coupled THM processes, fractured rock, partially saturated, geomechanics, Yucca Mountain, modeling, in situ experiments

ABSTRACT

[1] In this paper, we review data, findings, models, and analyses related to multiphysics processes—in particular coupled thermal, hydraulic, and mechanical (THM) processes—in partially saturated fractured rock from site investigations at Yucca Mountain, Nevada. We first review laboratory data and underground geologic mappings that form the basis for deriving *in situ* rock mechanical properties; these properties are central for analyzing multiphysics behavior of fractured rock masses. This is followed by a summary of findings from modeling and analysis of several major *in situ* experiments relevant to the conceptual understanding of thermally driven multiphysics in partially saturated fractured rock. We then summarize a few modeling studies of how THM multiphysics influence underground excavation stability and fluid flow. We conclude that the Yucca Mountain site investigation has provided us with an outstanding data set, one that has significantly advanced our knowledge of multiphysics processes in partially saturated fractured geological media. Such advancement was made possible, foremost, by substantial investments in multiyear field experiments that enabled the study of thermally driven multiphysics and testing of numerical models at a large spatial scale. The development of coupled-processes models within the project have resulted in a number of new, advanced multiphysics numerical models that are today applied over a wide range of geoscientific research and geoengineering applications. Using such models, the potential impact of THM multiphysics processes over the long term (e.g., 10,000 years) could be predicted and bounded with some degree of confidence. The fact that the rock mass at Yucca Mountain is intensively fractured enabled continuum models to be used, although discontinuum models were also applied and they are better suited for analyzing some issues, especially those related to predictions of rockfall within open excavations. The work showed that *in situ* tests (rather than small scale laboratory

experiments) are essential for determining appropriate input parameters for multiphysics models of fractured rocks, especially related to parameters defining how permeability might evolve under changing stress and temperature. A significant laboratory test program at Yucca Mountain also made important contributions to the field of rock mechanics, showing a unique relation between porosity and mechanical properties, a time dependency of strength that is significant for long-term excavation stability, a decreasing rock strength with sample size using very large core experiments, and a strong temperature dependency of the thermal expansion coefficient for temperatures up to 200°C. The analysis of *in situ* heater experiments showed that fracture closure/opening caused by changes in normal stress across fractures was the dominant mechanism for thermally-induced changes in intrinsic fracture permeability during rock mass heating/cooling, and fracture shear dilation appears to be less significant. The thermally-induced changes in permeability during heating/cooling of the rock mass stayed within one order of magnitude whereas excavation induced changes in permeability of up to two orders of magnitude could occur around tunnel openings. Significant effort was devoted to predicting the long-term stability of underground excavations under (mechanical) strength degradation and seismic loading, perhaps one of the most challenging tasks within the project. We note that such long-term strength degradation is actually an example of a chemically mediated process governed by underlying (microscopic) stress corrosion and chemical diffusion processes. In the Yucca Mountain Project, such chemically mediated mechanical changes were considered implicitly through model calibrations against laboratory and *in situ* heater experiments at temperatures anticipated to be experienced by the rock. A future possible research direction would be to simulate such processes mechanistically in a complete multiphysics THMC framework.

ACRONYMS AND ABBREVIATIONS

DST	Drift Scale Test
ECRB	Enhanced Characterization of the Repository Block
ERT	Electric resistivity tomography
ESF	Exploratory Studies Facility
GPR	Ground-penetrating radar
LBT	Large Block Test
NTS	Nevada Test Site
RMR	Rock Mass Rating
SHT	Single Heater Test
TH	thermal-hydrological
THC	thermal-hydrological-chemical
THM	thermal-hydrological-mechanical
THMC	thermal-hydrological-mechanical-chemical
TM	thermal-mechanical

Geological Abbreviations

CHn	Calico Hills and Lower Paintbrush nonwelded TM unit
PTn	Upper Paintbrush Tuff nowelded TM unit
TCw	Tiva Canyon welded TM unit
Tptpmn	Topopah Spring tuff middle nonlithophysal unit
Tptpll	Topopah Spring tuff lower lithophysal unit
Tptpnl	Topopah Spring tuff lower nonlithophysal unit
Tptpul	Topopah Spring tuff upper lithophysal unit
TSw	Topapah Spring welded
TSw1	Topopah Spring densely welded devitrified lithophysal-rich TM unit
TSw2	Topopah Spring densely welded devitrified lithophysal-poor TM unit

1 INTRODUCTION

[2] Multiphysics, including couplings between thermal, hydrological, mechanical and chemical (THMC) processes in geological media are critically important in natural geological processes and for a wide range of geological engineering practices, including geologic storage of nuclear waste, geologic carbon sequestration, geothermal energy extraction, as well as oil and gas extraction [Tsang 1987; 1991; 1999; Neuzil 2003; Rutqvist et al., 2001a; Rutqvist and Stephansson, 2003; Rutqvist, 2012]. Such multiphysics processes can be particularly strong and complex in fractured geological media, and even more complex under multiphase flow conditions and at high temperatures [Tsang et al., 2009b]. The most comprehensive and outstanding research and development related to multiphysics in fractured and partially saturated geological media—including multiphase flow and high temperature—have been conducted associated with the Yucca Mountain Project, Nevada, U.S.A. This research and development spans over 30 years and include development of various numerical models of increasingly complex physics, along with data arising from experiments, showing the importance of considering multiphysics processes and their couplings.

[3] The research and development related to multiphysics in fractured rocks around Yucca Mountain started in 1977 with the Nevada Nuclear Waste Storage Investigation Project that was established to evaluate geological formations for possible disposal of high-level radioactive waste on or adjacent to the Nevada Test Site (NTS). From 1977 to 1978, a number of geological settings and media—including alluvial, granite, argillite, and tuff—were examined. During these early efforts, a first study of coupled thermal-mechanical (TM) processes in tuff was made for a potential repository in a saturated unit, below the groundwater table [Tyler, 1980].

[4] In the early 1980s, the Topopah Spring welded (TSw) tuff unit located in Yucca Mountain, several hundred meters above the water table, was selected as the target unit for an unsaturated zone repository alternative (Figure 1). Excavation stability and TM impact were important factors in the selection of the TSw among several welded or nonwelded tuff units found at the site. Several near-field and far-field TM numerical analyses were performed [Johnson, 1984; Thomas, 1984; Melo and Parvish, 1984; Johnstone et al., 1984] using TM rock properties measured *in situ* or on samples extracted from vertical boreholes and outcrops in and around the NTS. It was concluded that, with respect to excavation stability, the welded tuff units were superior to the alternative nonwelded tuff units. In nonwelded tuff, drift stability problems could occur, because of its relatively low rock strength and the potential dehydration of clay minerals that would occur at high temperatures [Johnstone et al., 1984]. The welded TSw unit, on the other hand, is a hard, competent rock, in which the clay content is not significant enough to alter its mechanical properties.

[5] The unsaturated zone repository concept developed at Yucca Mountain was unique among the nuclear waste programs around the world. The repository tunnels would be open (not backfilled), situated several hundreds of meters above the water table, having the advantage of a capillary barrier that diverts liquid flow around the tunnel openings. The repository was designed such that the radioactive decay heat from the spent fuel would give rise to temperatures in the repository above the boiling point of water for hundreds of years. This would give rise to strong thermally driven multiphysics processes in the near field that would be expected to peak several hundred years after emplacement. Here, the near field may be defined as about one or two tunnel diameters from the tunnel wall, and far field at distances in the rock beyond this. From a repository performance perspective, these thermally driven processes are relatively short lived,

but complex, involving coupled multiphase fluid flow and heat transport, as well as geomechanical changes, especially close the drift walls where the temperature and stress would be the highest (Figure 2a). It was deemed important to understand these processes in detail and how they could impact long-term flow and transport properties, particularly around emplacement tunnels, and how they might impact the potential for water seepage into the tunnels (Figure 2b).

[6] It was recognized early on that TM evaluation only might not be sufficient; analyzing the long-term behavior would have to include the multiphysics of fully coupled thermal-hydrological-mechanical (THM) processes, or even coupled THMC processes, where C represents coupling to chemistry. It was also recognized that underground *in situ* experiments would be required for studying such processes *in situ* and for validating models at a relevant scale. Consequently, the first set of *in situ* heater tests in welded tuff was initiated already in the early 1980s, including an In Situ Tuff Water Migration/Heater Experiment [Johnstone et al. 1980; 1985], a set of small diameter heater experiments [Zimmerman, 1982, Zimmerman et al., 1986a], and a THM experiment on a 2 m cube heated block [Zimmerman et al., 1984, 1985, 1986b], all conducted in the G-tunnel located at Rainier Mesa within the NTS. These experiments provided the first *in situ* data on thermally driven multiphysics, in some cases involving above-boiling temperatures with evaluation of moisture transport and thermal stresses, as well as TM-induced changes in fracture aperture and permeability in the near-field rock. Such developments were also in line with nuclear waste programs worldwide, in which *in situ* experiments were already under way to study coupled processes, although mostly in saturated rock [Tsang, 1987].

[7] In 1987, the U.S. Congress decided to continue characterization of Yucca Mountain exclusively to evaluate its suitability to host a radioactive waste repository. A Site

Characterization Plan was completed in 1988 for systematic surface-based investigations, underground testing, laboratory testing, and modeling activities [DOE, 1988]. In the early 1990s, on behalf of the U.S. Nuclear Regulatory Commission, Manteufel et al. [1993] evaluated the potential importance of coupled processes at Yucca Mountain. This report, denoted NUREG/CR-6021, recommended further development of mathematical models and of well-documented experiments for coupled processes, and the validation of coupled models through comparison of model predictions and experimental observations. As recommended in NUREG/CR-6021, integrated large-scale *in situ* testing and numerical modeling became central for characterizing the fractured tuff within the Yucca Mountain Site Characterization Project.

[8] The construction in the mid 1990s of an 8-km long tunnel through Yucca Mountain, the Exploratory Studies Facility (ESF), was a critical development, because it allowed for underground mapping, development, and testing of rock engineering methods, and development of essential large scale *in situ* experiments (Figure 3). Among these experiments, the single heater test (SHT), initiated in 1996, followed by the Yucca Mountain Drift Scale Test (DST), initiated in 1997, were the most important efforts for developing conceptual understanding of thermally driven multiphysics at the Yucca Mountain.

[9] In the late 1990s, the ESF was complemented with the 2.7 km long Enhanced Characterization of the Repository Block (ECRB) Cross Drift, constructed through a stratigraphic unit embedded with lithophysae. The latter are cavities ("rock bubbles") caused by expanding gases in tuffs before solidification during formation of these geologic units. This was another important step, because nearly 80% of the then proposed repository was to be located in lithophysal-rich tuff units (Figure 3).

[10] Along with increased knowledge gained from the *in situ* testing, a number of numerical models for analysis of coupled TH, TM, and THM processes were developed, tested, and applied within the Yucca Mountain Project. At the Lawrence Berkeley National Laboratory, the computer code TOUGH was first adapted for the analysis of thermally driven multiphase fluid flow associated with a repository in partially saturated rock [Pruess and Wang, 1984]. The code would later be developed into the TOUGH2 code [Pruess et al., 1999], and extended with other TOUGH family codes that would be extensively applied throughout the Yucca Mountain Project. An alternative code called NUFT, developed at the Lawrence Livermore National Laboratory, was also extensively applied to model TH processes at Yucca Mountain from the early 1990s [Buscheck et al., 1996; 2003; Nitao 1998]. The TOUGH2 and NUFT codes were applied to develop models of the partially saturated fractured rock at Yucca Mountain based on the concept of multiple overlapping continua or dual-permeability, including flow properties for both fracture and matrix continua. The use of an overlapping continuum model added to the complexity of the numerical model, but offered the possibility of realistically partitioning flow between rock matrix and fractures. At the same time, additional TM analyses were conducted to study near-field TM effects for various repository designs [Arulmoli and St. John 1987; Johnson et al., 1989], as well as to evaluate changes in permeability at the mountain scale [Mack et al., 1989; Brandshaug, 1991; Jung and Ryder, 1993]. This was followed by a few TM studies related to the impact on near-field permeability evolution and drift seepage [Ho et al., 1998; Berge et al., 1999; Damjanac et al., 1999; Leem et al., 2005].

[11] In the final analyses to support a repository license application for authorizing construction of a Yucca Mountain repository, yet additional model approaches and codes were developed and applied. These included both continuum and discontinuum models for analysis of

various technical issues, such as drift design, long-term drift degradation, and THM effects on fluid flow [Lin et al., 2007; Damjanac et al., 2007; Rutqvist and Tsang 2003; Rutqvist et al., 2008a]. New coupled THM simulators were developed based on TH models such as NUFT and TOUGH2, extended to consider the impacts of geomechanical changes [Blair et al., 2001; Rutqvist et al., 2002]. These models were based on the dual-permeability concept inherent in the TH analysis, but were extended to include geomechanics. The models were then tested and validated against *in situ* experiments such as the SHT and DST [Rutqvist et al., 2005; Rutqvist et al. 2008a].

[12] The work at Yucca Mountain culminated in a license application submitted by the U.S. Department of Energy to the U.S. Nuclear Regulatory Commission in 2008. However, in 2010, the U.S. Administration issued a policy document stating that Yucca Mountain is no longer an option for consideration as the nation's civilian nuclear waste repository, and the Energy Department subsequently filed a motion to withdraw its application to store nuclear waste at Yucca Mountain [Carter et al., 2010; Tolefson, 2011].

[13] Nevertheless, the extensive studies over the 30 years up to 2008 at the Yucca Mountain site investigation have provided an outstanding data set and represented major scientific advances and technical achievements related to partially saturated fractured rock, including geomechanics and thermally driven multiphysics processes. Multiphysics, including coupled THM processes have been thoroughly investigated at Yucca Mountain, through large-scale, multiyear *in situ* experiments of dimensions and costs that are unlikely to be surpassed in the coming decades. It is important to compile and make this comprehensive data set, along with case studies and research findings, available to the scientific community, because these studies have yielded a fundamental, general understanding of coupled processes in fractured rock, as

well as an understanding of their influence on underground engineered structures. In this paper, we provide such a summary and review of the research and development related to the multiphysics associated with coupled THM processes, and believe that the extensive research findings will be of interest to a wide range of geoscientific disciplines and geoengineering applications.

[14] In this paper, we first provide an overview of how the conceptual understanding of the multiphysics related to coupled THM processes at the Yucca Mountain was developed and how this understanding was incorporated in the development of numerical models and analyses. Most of the material reviewed here is from published journal and conference papers, but we also include less-known work from project reports. We review laboratory data, underground geologic mappings, derivation of upscaled (*in situ*) rock engineering properties, and summarize research findings from several major *in situ* experiments. We then summarize a few modeling studies related to assessing how coupled THM processes influence underground excavation stability and fluid flow. The review is conducted from a geomechanics perspective, focusing on TM and THM processes. Pure TH processes have already been well documented by Tsang and Birkholzer [1999]; Birkholzer and Tsang [2000] and Tsang et al. [2009b], and THC processes [Spycher et al., 2003; Sonnenthal et al., 2005] are outside the scope of this review. We shall conclude this paper with some remarks on the potential importance of the full multiphysics framework, considering coupled THMC processes, including chemically mediated mechanical changes—an area we leave open for future research and development.

2 DEVELOPMENT OF CONCEPTUAL UNDERSTANDING AND MODELS

[15] As welded tuff units in the NTS were known to be heavily jointed, the first TM analyses of a potential repository at the Yucca Mountain were performed with continuum models to represent the fractured rock, accounting for preferred and non-uniform directionality [Tyler, 1980; Johnstone et al., 1984]. Since those early efforts, a lot was learned through substantial site investigations and modeling studies, which are briefly described in this section.

Findings from Laboratory Data

[16] Early laboratory studies of tuff samples from Yucca Mountain showed that porosity has a great effect on thermal and mechanical properties, but mineralogy and petrography have a relatively minor effect, although some minerals could affect the thermal expansion coefficient [Price, 1983, Price and Bauer 1985, Nimick 1988]. Based on the observation that thermal and mechanical properties could be directly related to porosity, a TM stratigraphic nomenclature was introduced by Ortiz et al. [1985]. The TM stratigraphy grouped rock with similar thermal and mechanical properties, and were intended to be used for drift design and rock engineering purposes. The TM stratigraphy designations of the rock layer to host the repository were the Topopah Spring densely welded devitrified lithophysal-rich (TSw1) TM unit, and the Topopah Spring densely welded devitrified lithophysal-poor rock (TSw2) TM unit.

[17] Empirical relationships that relate Young's modulus and unconfined compressive strength with porosity derived by Price and Bauer [1985] were important contributions to the field of rock mechanics, and they have had great practical significance for the Yucca Mountain Project. The data showed that the Young's modulus and unconfined compressive strength could

vary by more than one order of magnitude, depending on the sample porosity [Nimick 1988; Price et al. 1993, 1994] (Figure 4). Tests conducted at difference sample sizes showed that the elastic modulus and Poisson's ratio were independent of size, whereas compressive strength data decreased with size [Price et al., 1993]. Test conducted at different temperatures revealed no significant temperature effects on the short-term strength.

[18] The TM nomenclature was later partly phased out to make distinctions between subzones within the proposed repository units, including units with and without lithophysae. The subzones included four lithostratigraphic units at the level of the then proposed repository horizon, from top to bottom, the Topopah Spring tuff, upper lithophysal (Tptpul), middle nonlithophysal (Tptpmn), lower lithophysal (Tptpll), and lower nonlithophysal (Tptpnl) units (Figure 1b). The lithophysae-rich tuff consists of (1) matrix material, (2) vapor-phase mineral rims and (3) lithophysae, with lithophysae ranging in shape from circular to gashlike and in size from 1 to 100 cm (Figure 5a). Testing of lithophysal rock samples showed that the presence of lithophysae causes significant variability in the elastic (Young's) modulus and in the uniaxial (unconfined) compressive strength of tuff [Price 2004; Avar et al., 2003; Avar and Hudyma, 2007; Damjanac et al., 2007]. Some of these laboratory tests were conducted on large core samples (267–290-mm diameter) of the Tptpul and Tptpll units extracted from the ESF and Cross Drift, to be more representative of *in situ* conditions (Figure 5b).

[19] Tests conducted at different strain rates revealed a time dependency of mechanical properties [Martin et al., 1993, Ma and Daemen 2006]. Tests showed a strength decrease by about 10% for each order-of-magnitude decrease in strain rate from 10^{-5} to 10^{-9}, indicating moisture assisted stress corrosion [Martin et al., 1993]. Other tests conducted under constant stress reported by Martin et al. [1997] and Kicker et al. [2004], showed that the time to failure is

sensitive to differential stress (Figure 6). The data derived from these tests were analyzed in terms of static fatigue, and then used for calibration of creep models and evaluation of long-term strength degradation and stability of emplacement drifts [Lin et al., 2007; Damjanac et al. 2007].

[20] The thermal expansion coefficient has been extensively measured, both in the laboratory and *in situ*, since the early 1980s [Lappin, 1980; Schwartz and Chocas, 1992; Martin et al., 1996; Brodsky et al., 1997]. One distinct finding from these tests is that the thermal expansion coefficient is strongly temperature dependent (Figure 7). The strain for both nonwelded and welded tuff increases almost linearly until a “transition temperature” of approximately 150°C to 225°C is reached. In the case of welded tuff, the strain-versus-temperature curves become highly nonlinear at that point, with a dramatic increase in the thermal expansion coefficient. This increase is related to phase transition and the associated volume changes of some minerals, including cristobalite. In the case of nonwelded tuff, the dehydration of clay minerals (smectite and zeolite) tends to counteract thermal expansion at high temperatures. Thus, for any THM analysis involving this type of tuff, it is important to consider the temperature dependency of the thermal expansion coefficient.

[21] Natural fractures in samples extracted from many boreholes were tested for mechanical properties, as well as some hydraulic and hydromechanical properties (stress versus permeability). Peters et al. [1984] reported tests of fracture hydraulic conductivity as a function of normal stress. These tests showed the typical behavior of decreasing permeability with increasing normal stress, until residual permeability is attained at a normal stress of about 15 to 20 MPa. Thus, for normal stresses above 15 to 25 MPa, the fracture permeability remains practically constant. Much later, Constantino et al. [1999], conducting fluid-flow experiments

under changing normal stress on an artificial fracture in a 0.5 m scale block of welded tuff, found fluid flow to be insensitive to fracture normal stress up to 14 MPa.

[22] In the 1980s and early 1990s, a number of fractures were tested for mechanical properties (i.e. not involving fluid flow). These tests included determination of fracture normal and shear stiffness functions, shear strength, residual shear strength, and dilation angle at peak stress [Morrow and Byeflee, 1984; Olsson, 1987, 1988; Olsson and Brown, 1995]. In addition, fracture surface topography measurements were made with measurement techniques and analysis described by Brown [1995]. The roughness characteristics of the fracture surfaces derived from the profiles of these rock agree qualitatively with the simple mathematical model of Brown [1995], originally derived from fracture data in other rock types.

[23] Later, direct shear tests were performed on core samples containing internal fracture surfaces from the Tptpmn unit [Kicker et al., 2004]. Two tests were performed on subvertical cooling joints, and three tests were conducted on more or less horizontal vapor-phase partings. The two cooling joints were smooth, with an estimated Joint Roughness Coefficient (JRC) of 1 and 2, resulting in a cohesion of less than 0.08 MPa and a friction angle of about 33° to 34° [Kicker et al., 2004]. The three vapor-phase partings were rough, with an estimated JRC of 10 to 16, resulting in a cohesion of 0.66 to 0.84 MPa and a friction angle of 41.9° to 45.7°. Thus, shear characteristics for the smooth cooling joints and rough vapor-phase partings were found to be significantly different.

[24] In summary, the large number of laboratory tests that have been conducted since the late 1970s have been important for developing an understanding of the fundamental behavior and properties relevant to multiphysics processes in unsaturated tuff. In particular, the results for

Yucca Mountain tuff indicated that the following key findings should be considered when developing multiphysics THM models involving mechanical coupling in fractured volcanic tuff

- Porosity is the dominant factor in determining intact-rock mechanical properties and can be measured easily and used as a predictive tool for mechanical properties.
- The thermal-expansion coefficient of intact rock can be strongly temperature dependent.
- The strength of intact rock is scale dependent with decreasing strength for increasing size.
- There is a time-dependent effect on intact-rock strength that may be significant for analysis of long-term drift stability.
- The permeability of rock fractures can change dramatically as a result of stress induced changes in fracture aperture.
- There is a distinct difference in the shear behavior of smooth cooling joints and rough vapor-phase partings.

[25] These were findings derived for the volcanic tuff at Yucca Mountain, but some are also relevant other types of rocks. For example, in the case of relatively high porosity rocks such as shale and sandstone, the porosity can generally be used as an indicator of mechanical properties [Zoback, 2007]. The scale and time dependent effects on rock strength as well as the strong effects of stress on fracture permeability have also been observed in other types of rocks [Jaeger et al. 2007; Rutqvist and Stephansson, 2003].

Findings from Underground Mappings

[26] Fracture characteristics at Yucca Mountain were determined from data collected in underground excavations, borehole structure logs, and surface (outcrop, pavement) mapping

studies [Lin et al., 1993; Sweetkind et al., 1997; Nieder-Westermann, 1998; Mongano et al., 1999]. By far, the best and most abundant data description at Yucca Mountain came from Full-Periphery Geologic Maps (FPGMs) and Detailed Lines Survey (DLS) of the underground tunnels: ESF and Cross Drift [Nieder-Westermann, 1998; Mongano et al., 1999]. The FPGMs provides location and orientation (i.e., strike and dip) data, while the DSL data set contains information about fracture location, orientation, spacing, trace length, aperture, roughness, and mineralization along the tunnels.

[27] Underground fracture mapping along the ESF showed that for nonlithophysal rock (Tptpmn unit), three to four fracture sets could be identified. The three main fracture sets at the site are [Nieder-Westermann, 2000; Hinds, 2003; Maerz and Zhou, 2005]:

1. One prominent vertical, NW-SE trending, with median spacing of 0.22 m
2. One less prominent vertical, NE-SW trending, with median spacing of 1.01 m
3. One less prominent subhorizontal, with median spacing of 0.29 m

[28] Subvertical fractures, which represent almost 50% of the mapped fractures in the Tptpmn unit, often have curved surfaces with large-amplitude (dozens of centimeters) undulations and wavelengths of meters. These fractures often terminate in solid rock, leaving a solid rock "bridge" between adjacent rock fractures. The subhorizontal vapor-phase partings are relatively continuous structures filled with vapor-phase minerals. The surfaces are rough on a small scale and, as a result of the mineral filling, they have cohesion (unlike the subvertical fractures). In addition, there are randomly oriented fractures that account for about 30% of the mapped fractures in the Tptpmn unit. However, the aforementioned fracture statistics are based on mapping of fractures whose trace lengths are longer than one meter. Detailed-line surveys of

small-scale fractures were mapped at a few 6-m panels in the Tptpmn unit. That survey showed that the majority were small fractures with trace length shorter than one meter; fractures longer than one meter only accounted for less than 20% of all fractures at these locations [Kicker et al., 2004]. Thus, accounting for all fractures, the fracture spacing may be even smaller than the number quoted above.

[29] For the Tptpll unit, exposed in parts of the Cross Drift, similar fracture sets, two subvertical and one subhorizontal, were identified [Hinds 2003; Maerz and Zhou, 2005]. It was noted that lithophysal cavities commonly prevent propagation of medium-to-long-trace-length fractures, but small fractures connecting lithophysal cavities are abundant [Hinds et al., 2003]. Furthermore, core-drilling through the Tptpmn and Tptpll units show that the Tptpll unit was characterized by consistently higher core losses. In addition to the abundant small-scale fracturing in the Tptpll unit, the effect of lithophysal porosity indicates that rock quality and rock-mass strength could be significantly lower.

[30] We conclude that fracture mappings conducted at the Yucca Mountain site have shown that the once proposed repository units are intensively fractured, forming a well-connected fracture network [Hinds et al., 2003]. An intensively fractured rock implies that continuum models may be applicable for analysis of the multiphysics associated with coupled THM processes. In the fields of rock mechanics and hydrogeology it is known that if the fracture spacing is small compared to the characteristic dimension of the problem (e.g., the size of a drift), there is a better chance to derive representative average properties of the rock mass. Other types of hard rock might be sparsely fractured, such as crystalline fractured rocks at site like the Äspö Hard Rock Laboratory in Sweden, the Grimsel Test Site in Switzerland, and the Underground Research Laboratory (URL) in Manitoba, Canada (Rutqvist and Stephansson,

2003). In such case 90% of the fluid flow might go through a few open fractures and continuum representation might not be sufficient. However, as will be detailed below in this paper, at the Yucca Mountain, the practical use of continuum models was demonstrated for complex multiphysics processes and it turned out to be a sufficiently accurate approximation in this case. Finally, it was found that in the Tptpll unit, lithophysal cavities, and the small-scale fractures connecting the lithophysal cavities, have a significant effect on the mechanical rock-mass behavior [Kicker et al., 2004]. Thus, it shows that even small fractures can be important for the multiphysics behavior of fracture rocks, especially if they are abundant and well connected.

Derivation of Rock-Mass Mechanical Properties

[31] As part of the Yucca Mountain Site Characterization Project, empirical rock engineering methods were utilized for designing drifts and ground support. These methods use mapped distributions of fracture characteristics and intact rock properties to derive values for rock mass mechanical properties, including deformability and strength. However, the derived mechanical properties were not only used for drift design and ground support analysis; they were also used as input to coupled TM and THM models. At Yucca Mountain, these empirical methods were first used by Langkopf and Gnirk [1986] for the tuff repository unit evaluation, and the later was further developed by Hardy and Bauer [1991] for use in drift design, and finally were comprehensively applied by Lin et al. [1993].

[32] Because of the nature of fracture-mapping data, the rock mass empirical parameters and properties were classified into five quality categories correspond to a cumulative frequency occurrence of 5%, 20%, 40%, 70%, and 80%, respectively. The five rock-mass-quality categories provided a basis for ground-support design at different levels of confidence. The rock

mass was characterized by a range of parameters, estimated using both the rock mass quality (Q) and rock mass rating (RMR) indices. Also, rock-mass strength properties were evaluated in terms of several rock-mass failure criteria (e.g., Hoek and Brown [1982]), as well as in terms of approximate Mohr-Coulomb strength parameters (e.g., Lin et al., [1993] and Kicker et al. [2004]).

[33] The empirical methods and estimates of rock-mass properties evolved over the years, as new information became available, in particular from the ESF and later from the Cross Drift. In 1997, the rock-mass properties used for the ESF design confirmation were developed using two new indices, the Geological Strength Index (GSI) and the Rock Mass Index (RMI). However, the values derived for rock-mass strengths were difficult to confirm with field observations, generally because no rock failure was observed in the supported underground excavations at Yucca Mountain. Nevertheless, a few *in situ* experiments and observations were helpful in confirming and validating the empirical methods and estimated rock mass properties. For example, empirically derived values of rock-mass modulus could be compared to *in situ* results determined using pressurized slot and plate-loading tests (e.g., Zimmerman et al. [1989] and George et al. [1999]). In general, a deformation modulus of about 50% of the intact rock was found to be a reasonable average value for the nonlithophysal rock of the Tptpmn unit. Moreover, at the DST site, some minor fallout of rock chips from the drift crown could be used for estimating an *in situ* spalling strength of about 1/3 of the uniaxial compressive strength for small scale core samples of the Tptpmn unit [Rutqvist, 2004; Kicker et al., 2004].

[34] For lithophysal rock, yet a new set of rock-mass properties was derived and applied in the analysis of long-term degradation of excavations [Kicker et al., 2004]. This derivation used data from the earlier observations of porosity dependency of Young's modulus and uniaxial

compressive strength (Figure 4). However, experimental results at different scales were utilized, including the pressurized slot tests, as well as observations of fracturing in the side-walls of the ESF and Cross Drift (Figure 8). Moreover, the effect of the distribution, size, and shapes of the lithophysal cavities were analyzed using a discontinuum numerical model [Damjanac et al., 2007, Costin et al., 2009]. Test results were subdivided into five categories, based on five MPa increments of unconfined compressive strength. The strength and Young's modulus, as well as approximate equivalent lithophysal porosity, were then evaluated for each category. Figure 9 presents the ultimate rock-mass strength as a function of porosity, including results from large core-sample tests as well as pressurized slot tests [Costin et al., 2009]. The pressurized slot test results indicated a low deformation modulus, and these were consistent with the general relationships between strength, modulus, and porosity as observed in large-scale core laboratory tests [Kicker et al., 2004, Damjanac et al., 2007].

[35] Summarizing, the rock-engineering empirical methods were an integral part of drift design at Yucca Mountain, and these methods were tested and improved during the construction of the ESF and Cross Drift. The development of rock-mass mechanical parameters for the lithophysal rock was an important and necessary step, because of its distinctly different mechanical properties. Mechanical rock-mass properties developed by these methods were then consistently used for the various THM evaluations associated with the intended repository at Yucca Mountain, including analyses of TM effects on drift design, long-term drift-degradation analysis, and coupled THM analyses. The most important key finding from the development of rock mass engineering properties is the clear scale dependency in rock strength and deformability, indicating that the multiphysics associated with coupled THM processes must be

studied *in situ* at a relevant scale for model calibration and validation, leading at the end to a more confident prediction of long-term performance.

The G-Tunnel Heated Block Test

[36] The G-tunnel heated block test was an *in situ* THM experiment in partially saturated welded tuff conducted in the early 1980s, in the G-tunnel at Rainier Mesa, within the NTS [Zimmerman, 1982; Zimmerman et al., 1984, 1985, 1986b]. A 2 m cube block was produced by cutting slots in the floor of a drift in the G-tunnel (Figure 10). Two flatjacks were installed on each of the four sides of the block to provide mechanical load. The block was cut so that the two dominant sets of joints in the region were oriented approximately 45° to the loading axes. Heaters installed in the floor outside the block provided heating for the block. A single fracture within the block was isolated for flow testing. Many types of measurement instrumentation were installed. For analysis of THM processes, the most relevant measurements were temperature, displacement, and changes in fracture permeability. Deformation data for determination of thermal-expansion characteristics were obtained from four horizontal surface extensometers and two multiple-point extensometers. Changes in fracture permeability were measured on the isolated fracture by steady-state water injection.

[37] The results of the heater experiments showed that the thermal-expansion coefficient, under a constant bi-axial stress of 10.6 MPa, had a range of $(5.0 \text{ to } 8.7)\times10^{-6}$ C^{-1}, values that compared well with the laboratory range of $(6.4 \text{ to } 8.0)\times10^{-6}$ C^{-1}. The experiment also indicated that single fracture permeability was relatively insensitive to stress and only slightly sensitive to temperature increase under representative *in situ* conditions. The entire range of permeability change during the experiment was within one order of magnitude, with most changes occurring

during the excavation of the block (Figure 11). Results of loading and unloading under isothermal conditions indicated that the *in situ* rock-mass modulus considering the observed fracture deformation is about half the intact value, which ranges from 25 to 30 GPa [Zimmerman et al., 1985, 1986b].

[38] Costin and Chen [1988, 1991] analyzed the mechanical behavior of the G-tunnel heated block experiment using a continuum-based compliant-joint rock-mass model [Bauer and Conley, 1987; Chen 1986] and the finite element code JAC developed at Sandia National Laboratories. In this model, the rock was represented by two orthogonal sets of parallel, regularly spaced joints. A nonlinear normal stress-displacement and a bilinear shear-displacement model were used for fractures in each set for calculating the continuum stress-strain responses. A good quantitative agreement between experimental and numerical results was obtained in most cases, including an apparent irreversible shear slip behavior (Figure 12). Costin and Chen [1988] concluded that the continuum assumption appeared to be adequate in this experiment, in which the joint spacing was on the order of 15% of the nominal block size.

[39] For development of the conceptual understanding of THM multiphysics processes at Yucca Mountain, key findings from the G-tunnel heated block experiment showed that:

- The in situ thermal expansion coefficient is similar to that of intact rock.
- Measured fracture permeability changes during excavation and heating are within one order of magnitude.
- The in situ deformation modulus is about half that of intact rock.
- Irreversible displacement due to shear slip occurred during loading.
- The continuum assumption appears to be adequate for the scale of the block.

[40] Again, although these findings were derived for volcanic tuff, they would likely apply to other types of fractured rocks having the similar degree of fracturing, such as highly fractured granite or sandstone and below we will see that similar findings were obtained at other *in situ* heater experiments at Yucca Mountain.

The Single Heater Test

[41] In 1996, the first *in situ* heater test at Yucca Mountain, the Single Heater Test (SHT), was initiated. It was conducted in a side alcove of the ESF, in what would become the thermal test facility (Figure 3). Among a multitude of multiphysics data collected, the SHT provided data and information on the rock-mass hydrologic, thermal, and mechanical properties, as well as information on ground support/rock interaction at elevated temperature [Blair et al., 1998; Tsang et al. 1999]. The test was located in a large pillar exposed on three sides by drifts (Figure 13). A 5-m long horizontal heater was operated for 9 months. Temperature measurements showed that a dryout region (>100 °C) extended approximately 0.9 m into the rock from the heater. TM instrumentation, installed within and on the rock mass surrounding the SHT, included temperature measurements using thermocouples, RTDs and thermistors; displacement measurements using multiple-point boreholes extensometers, tape extensometers, and surface mounted wire extensometers; load measurements from load cells on rock bolts installed both within the thermally perturbed and ambient regions; and rock-mass-modulus measurements using a borehole jack.

[42] Both TM and TH pre-test analyses were conducted prior to the start of the SHT. A pre-test coupled TM analysis was conducted using the JAC3D code (a three-dimensional version of the JAC code used previously for modeling of the G-tunnel heated block test) and assuming a

linear elastic rock mass behavior [Finley et al., 1997]. In general, a reasonably good agreement between the calculated and measured displacements at the SHT was found using the intact-rock value of thermal expansion coefficient. Evolutions of predicted and measured displacements were similar, although absolute magnitudes could differ somewhat. However, while the numerical solution displayed smooth behavior, the measurements frequently indicated much more complex behavior, including apparent "stick-slip" events, which would be difficult to predict in detail (Figure 14). Still, we may say that the overall TM responses were reasonably well captured using a thermal-elastic model. Moreover, investigations of core samples taken before and after heating showed that the nine-month thermal exposure had no significant impact on long-term TM properties of intact rock [Brodsky and Barker, 1999].

[43] The TH analyses of the SHT showed typical development of a dryout zone corresponding to a super-heated (above boiling temperature) zone around the heat source within which moisture was driven out by the heat (Figure 15). Tsang and Birkholzer [1999] correlated the evolution of this dryout zone with measured evolution of air-permeability in the fractured rock mass. At the SHT, during the 9-month-heating and subsequent 4-month-cooling periods, air-injection tests were conducted in a few boreholes at time intervals of about two to four months. Two borehole sections located within a few meters from the heater showed a decrease in air permeability during the first three months of heating (Figure 16). During this time, the permeability decreased to between 25 to 50% of its original value. After cooling, the permeability recovered and actually exceeded the original value by a factor of 2 to 3 [Cho, 1999]. These changes in air permeability were well within one order of magnitude and were attributed to changes in fracture moisture content as a result of thermally driven water movement. However, judging from the results of the THM analysis of the Drift Scale Test to be described below, it is very likely that fracture closure

caused by TM effects have significantly contributed to these permeability changes. At the time, no fully coupled THM analysis was conducted for SHT, although attempts were made to relate potential increases in permeability caused by shearing to geophysical measurements [Blair et al., 1999].

[44] For development of the conceptual understanding of THM multiphysics processes in fractured tuff, the key findings from the SHT experiments are that:

- In situ deformation modulus is considerably lower than that of intact rock and appears to increase toward the intact value with increasing temperature and thermal stress
- The general behavior (trends and magnitude) of bulk rock mass thermal expansion can be reasonably well captured with a thermal-elastic continuum model and an intact rock thermal expansion coefficient.
- Although the general behavior could be captured with the thermal-elastic continuum model, there are also components of complex inelastic and fracture stick-slip behavior that cannot be readily predicted in detail.
- Near the heat source, combined TH and TM induced changes in fracture air permeability, first decreases permeability during heating to 25 to 50% of its original value, and then increases permeability during cooling by a factor of 2 to 3 of its original value. Thus, permeability changes as a result of the heating of the rock are well within one order of magnitude.

[45] These are in agreement with earlier findings at the G-Tunnel Heated Block Test regarding TM behavior in which the rock mass modulus is lowered by the compliance of fractures, intact rock thermal expansion coefficient applies, as well as the fact that permeability

changes stays within one order of magnitude. A thermal expansion coefficient close to intact rock has also been observed in modeling of other heater experiments in fracture rocks, including the Kamaishi Mine heater experiment in Japan [Rutqvist et al. 2001b], and the FEBEX in situ experiment at the Grimsel test site in Switzerland [Alonso et al., 2005]. This is because thermal expansion of the rock mass is controlled by the thermal expansion of the intact (matrix) rock between fractures, even in a highly fractured rock mass.

The Large Block Test

[46] A Large Block Test (LBT) was conducted at Fran Ridge, near Yucca Mountain in 1997 and 1998 [Lin et al., 2001; Blair, 2001; Wagner, 2002]. The LBT was designed to investigate rock-mass behavior in response to controlled boundary conditions. A block of fractured TSw tuff, measuring 3 m × 3 m in plane and 4.5 m high, was isolated in place by excavating the surrounding rock (Figure 17). Detailed geological mapping showed two subvertical sets of fractures and one set of subhorizontal fractures intersecting the block (Figure 17c). The two subvertical fracture sets were found to be approximately orthogonal, with 0.25 to 1 m fracture spacing, and a large number of smaller fractures were mapped as well (Figure 17c). A one-dimensional thermal field was created by using a plane heat source at a height of 1.75 m from the base of the block and placing heating/cooling coils on the top of the block. The block was heated for more than 12 months, from February 27, 1997, to March 10, 1998.

[47] TM measurements at the LBT included monitoring of the overall three-dimensional mechanical responses using six multiple-point borehole extensometers (Figure 17b). Three were oriented horizontally in the N-S direction; two were oriented horizontally in the E-W direction, and one was oriented vertically. Temperatures were monitored in vertical boreholes (one of

them, TT-1, is shown in Figure 17b). The measured horizontal displacements near the base of the block were small, essentially the same in the two horizontal directions, and they recovered close to zero during cool-down. The horizontal displacements near the top of the block were larger, isotropic, and only partially recovered. The vertical displacement was fairly small, but only partially recovered during cool-down [Wagner, 2002; Blair, 2001].

[48] Blair [2001] applied the distinct element code, 3-DEC [Cundall, 1988], to predict TM responses in the LBT. A series of simulations was carried out to calculate the responses as a function of the number of fractures and the coefficient of thermal expansion. The number of fractures included in the analysis varied from zero (solid intact rock) to 28 (all fractures with spacing about 0.25 to 1 m). Two values of thermal expansion coefficient were used: a high value of 9.73 °C^{-1} and a low value of 5.27 °C^{-1}. The analysis showed that displacement magnitudes were generally proportional to the value of the thermal expansion coefficient, whereas increasing the number of fractures had a relatively smaller impact, corresponding to an increased rock mass deformability. In general, the best agreement between calculated and measured displacement was achieved for vertical displacements and horizontal displacements near the base of the block, when using the lower value of the thermal expansion coefficient. In the upper part of the block, the displacements were generally underpredicted unless fractures were added, in effect reducing the rock mass modulus. One example is shown in Figure 18 for displacement along extensometer W2, located above the heat source. The lower value of thermal expansion coefficient (5.27 °C^{-1}) is slightly lower than the value for intact rock measured for the temperature range of 25 to 50°C (see Figure 7). Thus, it appears in this case that a thermal expansion coefficient slightly lower than that of intact rock was appropriate.

[49] Coupled TH analysis of the LBT by Mukhopadhyay and Tsang [2002] demonstrated the fact that while heterogeneity is a key issue for understanding and predicting flow and transport in fractured rock, strongly heat-driven processes tend to average out the effects of small-scale heterogeneity, so that a continuum representation is sufficient. In the LBT, fractures modeled as a homogeneous continuum could, in general, reproduce the temperature measurements which included heat pipe signatures, indicating a water and vapor counterflow. However, a storm event during the LBT resulted in temperature data showing a strong TH coupling, attributable to flow in large, discrete features of scale comparable to that of the block [Mukhopadhyay and Tsang, 2002].

[50] Some key findings from the LBT experiment are as follows:

- Considering the fractured heterogonous nature of the LBT, the continuum approach worked surprisingly well for modeling the multiphysics responses including complex and strongly heat-driven TH process and for TM processes, especially near the base of the bock where the rock mass was mechanically confined.
- The compliance of fractures is important in adding to rock mass deformability (resulting in a rock mass modulus considerable softer than intact rock modulus).
- Deformation in an unconfined fractured rock mass (such the upper part of the LBT) is much more challenging to model owing to loose blocks and wide open fractures and would probably be better represented in a discontinuous model.

[51] These findings generally agree with previous findings, but here the behavior of unconfined rock masses is added, which is more complex from mechanical perspective.

Niche Excavation Experiments

[52] Several niche excavation experiments were conducted to increase the understanding of excavation-induced permeability changes in the vicinity of drifts in partially saturated fractured tuff at Yucca Mountain [Wang et al., 2001; Wang and Cook, 2005]. The data were also used for calibration and validation of stress-versus-permeability models used in coupled THM analysis [Rutqvist, 2004]. A number of 10-m boreholes were drilled about 0.65 to 1 m above the planned drifts before their excavation. Then the drifts were excavated by a mechanical (alpine mining) method. Air permeability was measured before and after excavation in 30 cm packed-off sections along these boreholes, supposedly outside the excavation damaged zone (Figure 19a). The results showed that the permeability for individual measurements could increase by more than two orders of magnitude (Figure 19b).

[53] Analyses by Wang and Elsworth [1999] and Rutqvist and Tsang [2003] showed that the permeability increase could be explained by the opening of horizontal fractures unloaded by the drift. There was a tendency for stronger permeability increases in those sections where the initial permeability was small, a tendency also captured in the numerical analysis by Rutqvist [2004]. However, as shown in Figure 20, a plot of the permeability distribution before and after excavation of the niches indicates that the excavation-induced changes in permeability generally shift the permeability distribution to higher values, while the spread (standard deviation of log permeability) remains approximately constant. Furthermore, the excavation response for one niche in the more permeable Tptpll unit indicated a smaller increase in permeability.

Related to the Niche experiments, we like to mentioning two key findings, namely that

- Permeability close to the tunnel wall could increase by up to two orders of magnitude.

- There is a tendency for stronger permeability increases in those sections where the initial permeability was small, indicating a stronger permeability change in fractures with smaller initial aperture.

[54] Such tendency have also been observed by *in situ* hydromechanical experiments in fractured granite and could be related to that fractures with high initial aperture might be looked open by previously sheared having offset rough fracture surfaces [Rutqvist and Stephansson, 2003].

The Yucca Mountain Drift Scale Test

[55] The Yucca Mountain Drift Scale Test (DST) was a large-scale, multiyear rock-mass heating experiment designed to simulate the thermal loading that results from the emplacement of radioactive waste, albeit at an accelerated rate. It is the most important and successful effort at developing a conceptual understanding of thermally driven multiphysics processes at Yucca Mountain, and of partially saturated fractured rock in general. In fact, the multiphyscis of fully coupled THM processes in partially saturated fractured media were comprehensively studied and modeled for the first time as part of the analysis of the Yucca Mountain DST [Rutqvist et al., 2002, 2005], and furthermore the DST also provided data for coupled THC modeling [Sonnenthal et al. 2005].

[56] The DST was conducted in the thermal test facility adjacent to the SHT in the Tptpmn unit [Wagner, 2002], centered around a heated drift 5 m in diameter and 50 m long (Figure 21). Heating was provided by floor heaters along a 47.5 m long section of the heated drift, as well as by 50 rod heaters, referred to as "wing heaters," placed into horizontal boreholes emanating from, and orthogonal to, the heated drift (Figure 21). The wing heaters were included to account

for the horizontal conduction of heat from adjacent drifts in the repository layout. The DST, which started in 1997, included a four-year period of forced heating, followed by a four-year period of unforced (natural) cooling. A volume of over 100,000 m^3 of highly fractured volcanic tuff was heated, including several tens of thousand of cubic meters heated to above boiling temperature. This massive heating induced strongly coupled THMC changes and multiphysics that were continuously monitored by thousands of sensors embedded in the fractured rock mass.

[57] With respect to THM processes, measurements of temperature, deformation, and fracture permeability are the most relevant. At the DST, radial arrays of 20 m long boreholes drilled from the heated drift, and boreholes drilled parallel to the drift, were used for monitoring the temperature evolution (boreholes labeled "thermal" in Figure 21). In addition, deformation of the rock mass was monitored with an array of multiple-point borehole extensometer systems (boreholes labeled "mechanical" in Figure 21). Furthermore, periodic active air-injection testing was conducted to monitor changes in air permeability within the fracture system. These tests were conducted in clusters of 40 m long boreholes emanating from an observation drift and forming vertical fans that bracket the heated drift and the wing heaters (boreholes labeled "hydrology" in Figure 21). The air-injection tests provide a unique set of data, perhaps one of the most important data sets for constraining predictions of the coupled THM effects on permeability and fluid flow.

[58] Prior to the start of heating, predictive model simulations of coupled TH and TM processes were conducted using a number of different computer codes. These included three-dimensional simulations of TH processes conducted by Lawrence Berkeley National Laboratory using the TOUGH2 code [Birkholzer and Tsang, 1997, 2000] and by Lawrence Livermore National Laboratory using the NUFT code [Buscheck et al., 1997]. Coupled TM processes were

first simulated by the Sandia National Laboratories using the JAS3D code [Francis et al., 1997; Sobolik et al., 1998, 1999] and by Lawrence Livermore National Laboratory, using the 3-DEC code [Blair, 2001; Blair et al. 2001]. In the pre-test prediction of coupled TM processes Francis et al. [1997] applied a ubiquitously fractured continuum model approach that was based on previous experiences in modeling the SHT [Sobolik et al., 1998]. A reasonably good agreement between simulated and measured displacements during the heating phase confirmed the appropriateness of the continuum approach. The applicability of the continuum approach was also supported by results from a comparison between simulations using a discrete-fracture model and a continuum model by Blair [2001], which showed minor differences regarding mechanical displacements between the two approaches. It also indicated the dominance of thermo-elastic expansion within the rock matrix, although small local fracture slips may occur at certain locations.

[59] After the initiation of the DST, a new simulator named TOUGH-FLAC was developed to study the effects of THM multiphysics processes on hydrological properties and fluid flow in the unsaturated zone of Yucca Mountain. The TOUGH-FLAC simulator was built on a coupling between the TOUGH2 code [Pruess et al., 1999] and the widely used geomechanical code FLAC3D [Itasca, 1997]. In a TOUGH-FLAC simulation, the two computer codes—TOUGH2 and FLAC3D—are linked and jointly executed for coupled THM analysis under multiphase fluid flow conditions [Rutqvist et al., 2002; Rutqvist 2011].

[60] In 2002, the TOUGH-FLAC simulator was initially applied for a coupled THM analysis of the DST. The highly fractured rock mass was modeled as a dual-permeability medium. The effects of stress on hydraulic properties were analyzed using a conceptual model of a highly fractured rock mass that contained three orthogonal fracture sets. For each fracture set, using a

parallel-plate fracture flow model, a porosity correction factor (F_ϕ) and anisotropic permeability correction factors (F_{kx}, F_{ky}, F_{kz}) were calculated as a function of changes in normal stress across the fractures [Rutqvist 2004; Rutqvist et al. 2005].

[61] Figure 22 presents TOUGH-FLAC simulation results after 1 year of heating, showing a super-heated (above boiling temperature) zone around the drift in which moisture is driven out by heat. Figure 22a shows that the temperature has risen above the boiling point around the heated drift and near the wing heaters. High temperature induces strongly coupled TH processes with evaporation of liquid water and drying near the heat source (Figure 22b, dryout zone). The evaporated water is transported as vapor away from the heat source toward cooler regions, where it is condensed to liquid water (Figure 22b, dark blue). As a result, a dryout zone is created near the heat source and a condensation zone moves progressively away from the heat source.

[62] At the same time, the modeling showed that high temperature gives rise to thermal expansion of the rock mass with associated thermal stresses (Figure 22c). Near the heat source, the horizontal compressive stress increases strongly, with a maximum increase at the drift wall and near the wing heaters. Such an increase in compressive stress tends to tighten fractures to smaller apertures, leading to a reduction in air permeability. Away from the heat source, however, the horizontal stress decreases slightly. This reduction in horizontal stress allows pre-existing vertical fractures to open to a larger aperture, leading to an increase in air permeability in this area.

[63] Figure 22d shows the calculated THM-induced changes in air permeability. These changes are caused by the combined effect of TH-induced changes in fracture moisture content (Figure 22b) and TM-induced changes in fracture aperture (Figure 22c). That is, the total

permeability change factor caused by the combined TM and TH effects is calculated as $F_k\left(\Delta\sigma_x, \Delta S_l\right) = F_k(\Delta\sigma_x)\cdot F_{krg}(\Delta S_l)$ or $F_k^{THM} = F_k^{TM}\cdot F_k^{TH}$.

[64] Figure 22d shows that near the heat source, permeability decreases mainly because of fracture closure, but is also affected by TH-induced wetting and drying. Away from the heat source, about 20 m above the drift, a zone of slightly increased permeability has developed as a result of the opening of vertical fractures.

[65] The size and shape of the high temperature dryout zone (shown in Figure 22) were also monitored and inferred from geophysical methods, such as electric resistivity tomography (ERT), ground-penetrating radar (GPR) cross-hole tomography, and neutron logging [Wagner 2002; Tsang et al., 2009b]. Figure 23 shows ERT and GPR results in addition to recently interpreted seismic velocity data by Smith and Snieder [2010]. The GPR and ERT contours show a good correlation with the calculated extent of the dryout zone, mostly reflected by the drying of the rock matrix around the heat source. The seismic velocity model showed how wave speed changed through the superheated area. Smith and Snieder [2010] noted that the velocity change was lower than expected for water-to-steam conversion in saturated rock, and interpreted this as the lowering of velocity caused by thermally induced changes, such as thermal fracturing. However, we also like to mention the possibility that the decrease in wave velocity caused by water-steam conversion could have been partly offset by an increased rock bulk modulus as a result of fracture closure caused by the increased compressive stress in the superheated area.

[66] Figure 24 presents one set of comparisons of simulated and measured time-evolution of temperature, displacement, and permeability change factor [from Rutqvist et al., 2005]. Figure 24a shows excellent agreement between simulated and measured temperatures. Figure 24b

presents a comparison of the time evolution of rock-mass incremental displacements along six steeply inclined boreholes located at three different borehole arrays along the drift. The noticeable spread of the measured results may be attributed to rock-mass heterogeneities, such as fractures near measurement points. In the modeling, the rock is assumed homogeneous, so the predictions for all boreholes of the same type fall on the same line. Nevertheless, the simulated responses are within the range of the measured, indicating that the model captures the average displacements using the adopted material parameters. Sensitivity analyses showed that displacements are mainly dependent on the coefficient of thermal expansion, and to a lesser extent on the rock-mass deformation modulus. In this case, the use of a temperature-dependent thermal expansion coefficient derived from laboratory measurements on drill cores resulted in a good agreement between simulated and measured rock-mass thermal expansion.

[67] Figure 24c presents a comparison of simulated and measured fracture permeability in one borehole section where air-injection tests were conducted at regular time intervals of about three months. As mentioned, changes in air permeability are caused by the combined effect of TH-induced changes in fracture moisture content and TM-induced changes in fracture aperture. TM-induced changes in fracture permeability are controlled by thermal stress and the adopted stress-versus-permeability relationship. The stress-versus-permeability relationship is the most important input needed for predicting the evolution of fracture permeability. Obviously, if a more sensitive relationship between stress and permeability were adopted in the analysis, stronger changes in permeability would be predicted. The overall results for packed-off sections located at various locations around the heated drift showed that the model could predict reasonably well the magnitudes and trends of increasing or decreasing permeability values.

[68] The DST has also been a test case in the international cooperative project DECOVALEX (DEvelopment of COupled models and their VALidation against EXperiments) [Tsang et al., 2009a]. Within DECOVALEX, four research teams used four different numerical models to simulate and predict coupled THM processes at the DST [Rutqvist et al., 2005]. All used continuum model approaches but with slightly different model conceptualizations. Notable differences in the model approaches included different conceptualizations for mechanical analysis and for analysis of permeability changes. For example, some teams adopted elastic models, whereas others used elasto-plastic, or the so-called ubiquitous joint models, for analysis of the mechanical behavior. In general, the coupled THM responses were well captured by all teams, and TM-induced rock deformations were generally well simulated using an elastic model, although some individual displacements appear to be better captured using an elasto-plastic model.

[69] As far as the development of a conceptual understanding of multiphysics and coupled THM processes in fractured tuff is concerned, we conclude that the modeling of the DST experiment showed (consistent with previous findings at the G-tunnel, LBT, and SHT) that for the intensively fractured rock mass at the site, a continuum model approach is sufficient for simulating relevant coupled THM processes. Although some individual displacements appear to exhibit partly inelastic behavior, TM-induced rock deformations were generally well simulated using an elastic model and a temperature-dependent thermal expansion coefficient determined in the laboratory from intact rock samples. The results indicated fracture closure/opening, caused by changes in normal stress across fractures, is the dominant mechanism for TM-induced changes in intrinsic fracture permeability. Fracture shear dilation appeared to be less significant, at least during the active heating period. However, Rutqvist et al. [2008a] conducted a new more

detailed analysis of the DST, this time including the entire four-year period of forced heating and four-year period of unforced (natural) cooling. The new analysis included air-permeability data from over 700 pneumatic (air-injection) tests taken in 44 packed-off borehole intervals. By analyzing data from the entire heating and cooling cycle, it was possible to identify irreversible changes in intrinsic fracture permeability, consistent with either inelastic fracture shear dilation (where permeability increased) at some locations, or inelastic fracture surface-asperity shortening (where permeability decreased) at some other locations. According to Rutqvist [2009], it might be possible that such asperity shortening and associated decrease in fracture permeability might be enhanced by dissolution of highly stressed surface asperities over years of elevated stress and temperature.

[70] In summary, for development of a conceptual understanding of THM multiphysics processes in fractured tuff, the modeling of the DST experiment showed that:

- A continuum model approach is appropriate for simulating relevant THM multiphysics processes at the scale of a drift.
- Although some individual displacements appear to exhibit partly inelastic behavior, TM-induced rock deformations are generally well simulated using an elastic model and a temperature-dependent thermal expansion coefficient determined from intact rock samples.
- Fracture closure/opening caused by changes in normal stress across fractures is the dominant mechanism for TM-induced changes in intrinsic fracture permeability, and fracture shear dilation appears to be less significant at the DST.
- Some observed irreversible changes in intrinsic fracture permeability, could be consistent with either inelastic fracture shear dilation or inelastic fracture surface-asperity shortening.

- TM-induced changes in permeability at the DST, which are within one order of magnitude.

[71] In general, it is relevant to note that shear dilation appears to be relatively insignificant at the DST despite quite high shear stresses. It indicates that it is quite difficult to substantially increase permeability by shear in this case. This finding is relevant for the creation of Enhanced Geothermal Systems (EGSs), in which the main mechanisms for permeability enhancement would be shear. However, at Yucca Mountain, the rock mass was already highly permeable and some fractures might already have been fully dilated by previous shear events before the heating started. Nevertheless, the overall the permeability changes stayed within one order of magnitude as was also observed at the G-Tunnel heated block test and the SHT.

3 IMPACT OF THM MULTIPHYSICS ON UNDERGROUND EXCAVATIONS AND FLUID FLOW

[72] As part of the Yucca Mountain Project, a number of modeling studies were performed to evaluate the potential impact of THM multiphysics on underground excavations, fluid flow and transport associated with the then-proposed repository. Data from the above reviewed site investigations and experiments were used for deriving the multiphysics modeling input data, and the modeling studies are summarized and reviewed in this section.

Analysis of Stability of Underground Excavation

[73] In *Ground Control for Emplacement Drifts for SR* [Sun et al., 2001], stability issues were investigated for drifts subjected to *in situ*, thermal, and seismic load during the preclosure period for a repository at Yucca Mountain [Sun, 2001]. Thus, the analysis included thermal and mechanical effects on drift stability, but did not consider hydrological and chemical effects. The

final ground support for emplacement drifts was designed to include two systems: steel sets (1) with and (2) without fully grouted rock bolts, depending on the rock conditions (Figure 25).

[74] TM analyses were conducted to show that the support system could accommodate deformations caused by thermal loading, to ensure that induced stresses in the ground-support components would remain within allowable limits. Figure 25 (lower) shows an example of calculated axial force along rock bolts, using a continuum analysis with the FLAC3D code [Itasca, 1997]. The maximum axial tension force occurs in bolt 1 (see Figure 25 lower right) during thermal loading and is about 26 kN, which is well below the allowable tension force of 160.2 kN. It was therefore concluded that the fully grouted rock bolts could be designed for use in emplacement drifts, to provide the desirable functionality of preventing potential rock loosening and rock falls during the preclosure period, and that a satisfactory ground control system for the repository could be designed for a service life of up to 200 years [Sun, 2001].

[75] Very long-term stability, including rock strength degradation effects caused by stress corrosion (a hydrologic or chemical effect) was studied in the *Drift Degradation Analysis* [Kicker et al. 2004, Lin et al, 2007; Damjanac et al., 2007]. The analysis included estimates of rock-mass damage and changes in drift profile when subjected to loading from *in situ* stress, thermally induced stress, time-dependent strength degradation, and seismic ground motion.

[76] The *Drift Degradation Analysis* provided rockfall estimates in terms of particle size distribution, location, and impact velocity, as well as the total volume of rock particles displaced and the resulting static load of accumulated rubble within a collapsed drift. It also provided predictions of long-term changes in drift shape, which could impact the likelihood of water seepage into the drifts. Discontinuous (distinct element) models were applied in the *Drift*

Degradation Analysis to calculate progressive rock-mass failure with blocks falling out of the drift wall. Because of their distinctly different mechanical behavior, the *Drift Degradation Analysis* addressed stability for drifts located in lithophysal and nonlithophysal rock separately [Kicker et al., 2004; Lin et al., 2007; Damjanac et al., 2007].

[77] For drifts located in nonlithophysal rock [Kicker et al., 2004; Lin et al, 2007], a three-dimensional distinct element model was applied to analyze block structures around drifts, in which the interfaces between the individual blocks represent pre-existing macrofractures at the site. Time-dependent strength degradation was considered in terms of reduction in fracture shear strength parameters. A conservative estimate of this reduction was adopted by setting the strength parameters to represent residual shear-state parameters, considering that asperities on fracture surfaces had been sheared off. The analysis showed that thermal loading in nonlithophysal rock would stabilize the rock mass and reduce rockfall. The analysis also showed that the potential time-related fracture strength degradation has a minor impact on drift stability in nonlithophysal rock [Kicker et al., 2004; Lin et al. 2007].

[78] For drifts located in lithophysal rock [Kicker et al., 2004; Damjanac et al., 2007], a two-dimensional distinct element model was used to examine drift stability. In this case, the rock mass was represented as an assembly of polygonal, elastic blocks, bounded together across the intervening contact planes. The model was calibrated to reproduce the mechanical properties given by the range of five lithophysal rock-strength categories mentioned above. The impact of lithophysal spatial variability was assessed based on geologic mapping and stratiform geometry [Lin et al., 2005]. For analysis of time-dependent strength degradation, a time-dependent strength model was developed using the results from the static-fatigue laboratory tests shown in Figure 6. The approach taken was to assume that the rock-mass cohesion and tensile strength would be

reduced to zero in a brittle fashion at time of failure, defined by the slope of the static fatigue test results [Kicker et al., 2004; Damjanac et al., 2007].

[79] Figure 26 presents an example of the time-dependent degradation results for *in situ* and thermal stress conditions at 10,000 years. The figure shows that shear failure of the sidewalls is the failure mode observed for lithophysal rock strength Category 2, whereas yielding in the crown of the drift occurs for Category 5. This is a function of the location of the largest thermally induced stress component, which in turn, is a function of the Young's modulus for the rock mass. For a drift in the Category 5 rock, a higher Young's modulus gives rise to a higher thermal stress in the horizontal direction, which results in increased stress concentration at the top of the drift. The analysis further showed that an additional seismic shaking of the drifts by a high-probability event would result in a shake-down of microfractured and damaged material, with fragmented rock particle sizes on the order of centimeters to decimeters, but would not result in complete collapse of the drifts. Overall, the *Drift Degradation Analysis* showed that time-dependent strength degradation was not expected to be substantial for drifts located in typical lithophysal rock. Only for drifts located in the lowest rock quality (Category 1 and 2), representing less than 10% of the lithophysal rock mass, would some damage and rockfall be expected [Kicker et al. 2004; Damjanac et al. 2007].

Analysis of THM effects on fluid flow

[80] A drift-scale THM model analysis was conducted to investigate the impact of THM processes on hydrologic properties (permeability and capillary strength) and on flow in the near-field rock around a heat-releasing emplacement drift [Rutqvist 2004; Rutqvist and Tsang, 2003]. The case was later used as a benchmark calculation test in the DECOVALEX project,

involving four international teams [Rutqvist et al., 2008b; Rutqvist et al., 2009]. The analysis showed how the heat generated by the decay of radioactive waste would result in elevated rock temperatures for thousands of years after waste emplacement (Figure 27). Increasing temperature would cause thermally driven multiphysics processes in the near field as those observed and modeled at the SHT and DST, including thermal stresses that could cause mechanical and permeability changes in the excavation disturbed zone.

[81] The drift-scale coupled THM modeling was conducted with TOUGH-FLAC and built upon insight obtained in earlier studies involving a sequential-snapshot, one-way coupled approach using separate TH and TM analyses [Berge et al., 1999; Blair, 2001]. A bounding analysis was conducted that bracketed the potential impact of THM processes on hydrologic properties (including permeability) and the flow field [Rutqivst, 2004; Rutqvist and Tsang, 2003]. The bounding case was realized by adopting parameter values that emphasize the effects of the THM coupling. This included a bounding estimate of the thermal expansion coefficient by using the value determined from unfractured rock samples (emphasizing thermal stress) and a bounding estimate of a stress-versus-permeability function calibrated against the largest permeability changes observed in Yucca Mountain field experiments (emphasizing TM-induced permeability change).

[82] The drift-scale THM analysis showed that the maximum THM effects could occur around 100 to 1,000 years after waste emplacement, when the temperature in the rock mass at the repository level reaches its maximum. The primary THM effects includes thermally induced changes in the stress field that act on preexisting fractures, causing fracture closure or opening with accompanying changes in fracture permeability and capillary pressure. Using the bounding stress-versus-permeability relationship, the vertical permeability in the Tptpmn unit was

predicted to decrease by (at most) a factor of 0.03 from the original permeability. In the Tptpll unit, vertical permeability was predicted to decrease by (at most) a factor of 0.5 from the original value. However, the analysis indicated that the impact on the flow field would be relatively small, with the largest impact occurring for a repository located in the Tptpmn unit. As observed in Figure 28a, the main impact would be on the dryout zone near the emplacement drift [Rutqvist, 2004; Rutqvist et al., 2009]. When stress-induced changes in hydrological properties are considered, the extent of the dryout zone was found to be smaller. The simulation results showed that this shrinkage of the dryout zone was caused primarily by a significantly smaller fracture permeability, which reduced heat convection with gas flow and thereby reduced the heat-pipe effect, thus leading to an accelerated rewetting of the dryout zone. The analysis further showed that in the longer term (at around 10,000 years) the reduction in vertical permeability would still be significant, especially just above the emplacement drift. The impact of this reduction in permeability, however, was relatively small, and tended to prevent vertical flux from reaching the drift at the crown region (Figure 28b).

4 CONCLUDING REMARKS

[83] Since the first TM analyses were done in the late 1970s and early 1980s, the Yucca Mountain site investigation has significantly advanced the state of knowledge of THM multiphysics in partially saturated, fractured geological media. Significant efforts were devoted to study multiphysics *in situ* through multiyear field experiment to validate the various numerical models at a relevant scale. Using such models, the potential impact of coupled THM processes on the long-term repository performance could be predicted and bounded with some degree of confidence.

[84] Analyses of the Single Heater Test and the Drift Scale Test have been the most important contributions for developing the current conceptual understanding of THM multiphysics for the partially saturated, fractured tuff at Yucca Mountain. In particular, the innovative measurements of permeability changes through air-injection tests at DST have been crucial for the development of a model for analysis of THM multiphysics. The effect of THM on permeability would otherwise be very difficult to predict with the same level of confidence.

[85] The site investigation, from laboratory experiments, to field mapping and large scale *in situ* heater experiments resulted in a number of key findings relevant to the development of a conceptual understanding of THM multiphysics processes in fractured tuff. A significant laboratory test program made important contributions to the field of rock mechanics, showing a unique relation between porosity and mechanical properties, a time dependency of strength that is significant for long-term excavation stability, a decreasing rock strength with sample size using very large core experiments, and a strong temperature dependency of thermal expansion coefficient for temperatures up to 200°C. The analysis of *in situ* heater experiments showed that fracture closure/opening caused by changes in normal stress across fractures was the dominant mechanism for thermally-induced changes in intrinsic fracture permeability during rock mass heating/cooling, and fracture shear dilation appears to be less significant. The thermally-induced changes in permeability during heating/cooling of the rock mass stayed within one order of magnitude, whereas excavation induced changes in permeability of up to one order of magnitude could occur around tunnel openings.

[86] The fact that the rock mass at Yucca Mountain is highly fractured has enabled continuum models to be used for THM multiphysics analysis, although discontinuum models have also been applied and are better suited for analyzing some issues, especially related to prediction of

rockfall within open excavations. The predictions of long-term degradation of excavations and potential for rockfall under seismic loading were particularly challenging tasks, subjected to a high level of uncertainty. A significant effort was devoted to this task and the approach developed and applied in the Yucca Mountain Project can serve as model for future studies of the long-term behavior of underground excavation and fractured rock masses in general.

[87] Substantial advancements were achieved in the development of numerical models for the analysis of thermally driven multiphysics. The early developments and applications involved separate TH and TM process modeling, but such models were later merged together, enabling the analysis of coupled THM processes. Models were also developed and applied for analyzing coupled THC processes, including reactive transport. Such THC and THM models (and analyses) were developed and applied in parallel until the end of the Yucca Mountain Project, and not merged into a complete multiphysics THMC model or analysis. In terms of repository performance for the final license application, it was deemed unnecessary to conduct a fully coupled THMC analysis. In fact, there would probably not be enough data to obtain the necessary model parameters, including parameters for the coupling between mechanics and chemistry.

[88] Nevertheless, the development of coupled-processes models within the Yucca Mountain project have resulted in a number of new, advanced multiphysics numerical models that are today applied over a wide range of geoscientific research and geoengineering applications. For example, the TOUGH-FLAC simulator is now being applied to study THM multiphysics related to CO_2 sequestration [Rutqvist et al., 2010a; Cappa and Rutqvist, 2011], geothermal energy extraction [Rutqvist and Oldenburg, 2010b], naturally occurring CO_2 upwelling and crustal deformations [Todesco et al., 2004; Cappa et al., 2009], gas production from hydrate-bearing

sediments [Rutqvist and Moridis, 2009; Rutqvist et al., 2009], underground compressed air energy storage [Rutqvist et al., 2012], and nuclear waste disposal in bentonite-backfilled tunnels in granite or clay host rocks [Wang et al., 2011; Rutqvist et al. 2011]. Modeling these application benefits from the research and development at Yucca Mountain, because they require the analysis of multiphysics processes involving complex multiphase flow and geomechanics in geological media that may or may not be initially fractured.

[89] The site investigations related to the fractured rock multiphysics at Yucca Mountain showed the importance of *in situ* experiments for determining the appropriate input parameters for mutiphysics models. In particular, fractured rock permeability and how permeability might evolve with stress, fluid pressure, and heat could not be readily predicted based on laboratory experiments of small core samples. A very significant increase in aperture and permeability can be noted as a result of scale effects (or sampling biases) when comparing results from laboratory and *in situ* tests. The stress-versus-permeability models developed for the fractured rock mass at Yucca Mountain have been applied to other fields of application involving fractured rock masses. For example, at the In Salah CO_2 storage site, injection takes place into an intensively fractured but otherwise relatively tight sandstone reservoir [Rutqvist et al., 2010; Liu and Rutqvist, 2012]. An empirical exponential stress-versus-aperture relation that was used for in situ calibration of the THM models at Yucca Mountain [Rutqvist and Tsang, 2003] were later derived by closed form solutions and applied for the fractured reservoir at In Salah [Liu and Rutqvist, 2012]. In fact such an exponential relation—or modification thereof—have proven to be valid for a wide range of rock materials, including intact granite [Liu et al., 2009], clay stone [Liu et al., 2011], and coal [Liu and Rutqvist, 2010]. The knowledge on how permeability changes under changing normal and shear stress (in situ) is also highly relevant for the

development of EGSs. Indeed, the TOUGH-FLAC code and stress flow coupling functions developed for fracture tuff at Yucca Mountain have been applied for the modeling of the reservoir stimulation by cold water injection into geothermal reservoir under rock temperatures up to 400°C for the NW Geysers EGS demonstration project, in California [Rutqvist et al. 2010] as well as for the Newberry Canyon EGS demonstration in Oregon [Rinaldi et al. 2012]. Interestingly, the rock at Newberry Canyon is also volcanic tuff, but the intended EGS reservoir is much deeper, located at 2 to 3 km, having a much smaller initial rock mass permeability. However, the modeling approach for Newberry Canyon also involves an *in situ* calibration of a stress-versus-permeability function (using injection test data) and this is followed by a prediction of potential shear reactivation and permeability changes during the subsequent EGS stimulation.

[90] As a final remark, it can be pointed out that apart from the abovementioned strength degradation, there is also evidence [Rutqvist, 2009] of chemically mediated changes in fracture aperture and permeability, which has been observed in the controlled laboratory experiments for other types of rock [Yasuhara et al., 2004] as well as inferred from an *in situ* block test [Min et al., 2009]. This phenomenon involves fracture closure caused by pressure solution of contacting fracture surface asperities, a process that is enhanced under higher stress and temperature. At Yucca Mountain, such a phenomenon has been inferred from laboratory experiments [Lin and Daily, 1990], from observations at the G-tunnel *in situ* heated block experiment [Zimmerman et al., 1985], and the Yucca Mountain Drift Scale Test [Rutqvist et al., 2008a; Rutqvist, 2009]. However, because temperature and stress increase simultaneously, it is difficult to separate the pure thermal-mechanical responses from that of chemically mediated responses. Therefore, the back-calculated stress-versus-aperture functions would implicitly include additional fracture closure caused by chemically mediated changes. Similarly, static fatigue experiments used for

calibrating creep models in the drift-degradation analysis may also implicitly include underlying chemical processes. An explicit and mechanistic modeling of such phenomena would require full THMC multiphysics modeling, which is an avenue worth pursuing for future research.

ACKNOWLEDGMENT

[91] The work was supported by the Office of Civilian Radioactive Waste Management, Office of the Chief Scientist, of the U.S. Department of Energy under Contract no. DE-AC02-05CH11231. We thank Bill Arnold at Sandia National Laboratories, two anonymous reviewers, and the Associate Editor for constructive comments on the initial manuscript. Editorial review by Dan Hawkes of the Lawrence Berkeley National Laboratory is greatly appreciated.

5 REFERENCES

Alonso, E.E., J. Alcoverro, F. Coste F. et al. (2005) The FEBEX Bechmark test. Case Definition and comparison of modelling approaches. *Int. J. Rock. Mech. Min. Sci*, *42*, 61–638.

Arulmoli, K., and C. M. St. John (1987), Analysis of Horizontal Waste Emplacement Boreholes of a Nuclear Waste Repository in Tuff. *Rep. SAND86-7133*. Sandia Natl. Lab. Albuquerque, N. M.

Avar, B. B., and N. W. Hudyma (2007), Observations on the influence of lithophysae on elastic (Young's) modulus and uniaxial compressive strength of Topopah Spring Tuff at Yucca Mountain, Nevada, USA, *Int. J. Rock Mech. Min. Sci.*, *44*, 266–270.

Avar, B. B., N. Hudyma, and M. Karakouzian (2003), Porosity dependence of the elastic modulus of lithophysae-rich tuff: numerical and experimental investigations. rock, *Int. J. Rock Mech. Min. Sci.*, *40*, 919–928.

Bauer, S. J., and C. H. Conley (1987), A proposed method for predicting rock-mass deformability using a compliant joint model, in *Proceedings of the 28th US Rock Mechanics Symposium*, edited by I. W. Farmer, J. J. K. Daemen, C. S. Desai, C. E. Glass, and S. P. Neuman, University of Arizona, 29 June to 2 July 1, Balkema.

Berge, P. A., S. C. Blair, and H. Wang (1999), Thermomechanical effects on permeability for a 3-D model of YM rock, in *Proceedings of the 37th US Rock Mechanics Symposium*, edited by B. Amadei B, R. L. Kranz RL, G. A. Scott and P. H. Smeallie PH, Vail, Colorado, June 6 to 9.

Birkholzer, J. T., and Y. W. Tsang (1997), Pretest analysis of the thermal hydrological conditions of the ESF drift scale test, Rep. *LBNL-41044*, Lawrence Berkeley Natl. Lab., Berkeley, Calif.

Birkholzer, J. T., and Y. W. Tsang (2000), Modeling the thermalhydrologic processes in a large scale underground heater test in partially saturated tuff, *Water Resour. Res.*, *36*(6), 1431–1447.

Blair, S. C. (2001), Coupled Thermal-Hydrologic-Mechanical Effects on Permeability Analysis and Models Report. *ANL-NBS-HS-000037 REV 00*. Bechtel SAIC Company, Las Vegas, Nevada.

Blair, S. C., T. A. Buscheck, L. D. DeLoach, W. Lin and A. L. Ramirez (1998), *Single-Heater Test Final Report*. (*UCRL-LD-13 1491*), Lawrence Livermore National Laboratory, Livermore, CA.

Blair, S. C., W. Lin, A. L. Ramirez, W. D. Daily, and T. A. Buscheck (1999), Coupled THM analysis of the Single Heater Test at Yucca Mountain, in *Proceedings of the 37th US Rock Mechanics Symposium*, edited by B. Amadei B, R. L. Kranz RL, G. A. Scott and P. H. Smeallie PH, Vail, Colorado, June 6 to 9.

Blair, S. C., S. R. Carlson, and J. L.Wagoner (2001), Distinct element modeling of the drift scale test, in *Proceedings of the 38th US Rock Mechanics Symposium*, edited by D. Elsworth, J. P. Tinucci, and K. A. Heasley, Washington D.C., July 7 to 10.

Brandshaug, T. (1991), *A Thermomechanical Far-Field Model of Yucca Mountain*, *Rep. SAND 85-7101*, Sandia Natl. Lab., Albuquerque, N. M.

Brodsky, N. S., M. Riggins, and J. Connolly (1997), Thermal expansion, thermal conductivity, and heat capacity measurements at Yucca Mountain, Nevada, *Int. J. Rock Mech. Min. Sci.*, *34*, Paper No. 040.

Brodsky, N. S., and T. S. Barker (1999), Effect of Single Heater Test on intact rock properties at Yucca Mountain, Nevada, in *Proceedings of the 37th US Rock Mechanics Symposium*, edited by B. Amadei B, R. L. Kranz RL, G. A. Scott and P. H. Smeallie PH, Vail, Colorado, June 6 to 9.

Brown, S. R. (1995), Simple mathematical model of a rough fracture, *J. Geophys. Res.*, *100*, 5941–5952.

Buscheck, T. A., J. J. Nitao, and L. D. Ramspott (1996), Localized dryout: An approach for managing the thermal-hydrological effects of decay heat at Yucca Mountain, in *Scientific Basis for Nuclear Waste Management XIX*, edited by W. M. Murphy and D. A. Knecht, Mater. Res. Soc. Symp. Proc., 412, 715–722.

Buscheck, T. A., R. J. Shaffer, and J. J. Nitao (1997), *Pretest thermal-hydrological analysis of the Drift-Scale Thermal Test at Yucca Mountain*. *ACC: MOL.19980507.0359*, CRWMS M&O, Las Vegas, Nevada.

Buscheck, T. A., N. D. Rosenberg, J. A. Blink, Y. Sun, and K. Mansoor (2003), Analysis of thermohydrologic behavior for above-boiling and below-boiling thermal-operating modes for a repository at Yucca Mountain, *J. Contam. Hydro*l., *62–63*, 441–458.

Cappa F. and J. Rutqvist (2011) Impact of CO2 geological sequestration on the nucleation of earthquakes. *Geophysical Research Letter*, *38*, L17313.

Cappa, F., J. Rutqvist, and K. Yamamoto (2009) Modeling crustal deformation and rupture processes related to upwelling of deep CO2 rich fluids during the 1965-1967 Matsushiro Earthquake Swarm in Japan. *Journal of Geophysical Research*, *114*, B10304.

Carter, L. J., L. H. Barrett, and K. C. Rogers (2010), Nuclear waste disposal showdown at Yucca Mountain. Issues in Science and Technology Online, Fall 2010. 80-84. University of Texas, Dallas, http://www.issues.org/

Chen, E. P. (1986), Two-dimensional continuum model for jointed media with orthogonal sets of joints, *in Proceedings of the 27th US Rock Mechanics Symposium*, edited by H.L. Harman, University of Alabama, Tuscaloosa, June 23 to 25.

Cho, J. B. (1999), *Single Heater Test Final Report*. *BAB000000-01717-5700-00005 REV 00 ICN 1*. CRWMS M&O. Las Vegas, Nevada.

Constantino, M. S., S. C. Blair, and S. R. Carlson (1999), Fluid flow in 0.5-m scale blocks of Topopah Spring tuff, in *Proceedings of the 37th US Rock Mechanics Symposium*, edited by B. Amadei B, R. L. Kranz RL, G. A. Scott and P. H. Smeallie PH, Vail, Colorado, June 6 to 9.

Costin, L. S., and E. P. Chen (1988), An analysis of the G-Tunnel Heated Block Experiment using compliant-joint rock-mass model, in *Proceedings of the 29th US Symposium on Rock Mechanics*, edited by P.A. Cundall, R.L. Sterling, A.M. Starfield, University of Minnesota, Minneapolis, 13 to 15 June.

Costin, L. S., and E.P. Chen (1991), A thermomechanical analysis of the G-tunnel heated block experiment using a compliant-joint rock-mass model. *Int. J. Numer. Anal. Methods Geomech*, *15*, 379-398.

Costin, L. S., R. H. Price, and M. Y. Lee (2009), Characterization of a high lithophysal welded tuff unit using a multi-scale approach, in *Proceedings of the International Conference on Rock Joints and Jointed Rock Masses*, Tucson, Arizona, Jan 4 to 10.

Cundall, P. A. (1988), Formulation of a three-dimensional distinct element model—Part I. A scheme to detect and represent contacts in a system composed of many polyhedral blocks. *Int. J. Rock Mech. Min. Sci. & Geomech. Abstr.*, *25*, 107-116.

Damjanac, B., C. Fairhurst, and T. Brandshaug (1999), Numerical simulation of the effect of heating on the permeability of a jointed rock mass, in *Proceedings of the Congress of the International Society of Rock Mechanics 9*(2), 881-885.

Damjanac, B., M. Board, M. Lin, D. Kicker, and J. Leem (2007), Mechanical degradation of emplacement drifts at Yucca Mountain—A modeling case study. Part II: Lithophysal rock. *Int. J. Rock Mech. Min. Sci.*, *44*, 368–399.

DOE, (U.S. Department of Energy) (1988), *Site Characterization Plan Yucca Mountain Site, Nevada Research and Development Area, Nevada. DOE/RW-0199*. Nine volumes. U.S. Department of Energy, Office of Civilian Radioactive Waste Management, Washington D.C.

Finley, R. E., S. R., Sobolik, N. D. Francis, S. Ballard, J. T. George, and L. S. Costin (1997), Preliminary thermomechanical results of a heater test in welded tuff. *Int. J. Rock Mech. Min. Sci.*, *34*:3–4, Paper No. 080.

Francis, N. D., S. R. Sobolik, C. K. Ho, R. R. Eaton, and D. Preece (1997), *Pre-experiment thermal-hydrological-mechanical analyses for the ESF heated drift experiment. SLTR97-0002 CRWMS M&O*, Las Vegas, Nevada.

George, J. T., R. E. Finley, and M. Riggins (1999), Conduct of plate loading test at Yucca Mountain, Nevada, in *Proceedings of the 37th US Rock Mechanics Symposium*, edited by B. Amadei B, R. L. Kranz RL, G. A. Scott and P. H. Smeallie PH, Vail, Colorado, June 6 to 9.

Hardy, M. P., and S. J. Bauer (1991), *Drift Design Methology and Preliminary Application for the Yucca Mountain Site Characterization Project*, *Rep. SAND89-0837,* Sandia Natl. Lab., Albuquerque, N. M.

Hinds, J. J., G. S. Bodvarsson, and G. H. Nieder-Westermann (2003), Conceptual evaluation of the potential role of fractures in unsaturated processes at Yucca Mountain, *J. Contam. Hydrol.*, *62-63*, 111–132.

Ho, C. K., and N. D. Francis (1998), Coupled thermo-hydro-mechanical simulations of the potential repository at Yucca Mountain, in *Proceedings of the 9th International Conference on High Level Radioactive Waste Management Conference*, Las Vegas, Nevada.

Hoek, E., and E. T. Brown (1982), *Underground Excavation in Rock*, London, England: The Institute of Mining and Metalurgy.

Itasca, (1997), *FLAC-3D Manual: Fast Lagrangian Analysis of Continua in 3 Dimensions–Version 2.0.* Itasca Consulting Group Inc., Minnesota, USA, 1997.

Jaeger, J.C., N.G.W. Cook, and R.W. Zimmerman (2007), Fundamentals of rock mechanics (4th edition), Blackwell publishing, Malden, MA, USA.

Jung, J., and E. E. Ryder (1993), Thermal-Mechanical Analyses for the Yucca Mountain Project, in *Proceedings of the 34th US Rock Mechanics Symposium,* edited by B.C. Haimson, University of Wisconsin, Madison, June 28 to 30.

Johnson, R. L. (1984), *Unit Evaluation at Yucca Mountain, Nevada Test Site: Near Field Thermal and Mechanical Calculation Using the SANDIA ADINA Code, Rep. SAND83-9939*, Sandia Natl. Lab., Albuquerque, N. M.

Johnson, K. I., D. J. Sherwood, and C. F. Voss (1989), A sensitivity study of near-field thermalmechanical conditions in Tuff, in *Proceedings of the Topical Meeting on Nuclear Waste Isolation in the Unsaturated Zone; Focus 89*, American Nuclear Society, La Grange Park, IL.

Johnstone, J. K., and G. R. Hadley (1980), In situ tuff water migration/heater experiment, in *Proceedings of the 1980 National Waste Terminal Storage Program Information Meeting*, *ONWI 212*, Columbus, OH.

Johnstone, J. K., R. R. Peters, and P. F. Gnirk (1984), *Unit Evaluation at Yucca Mountain, Nevada Test Site: Summary Report and Recommendation, Rep. SAND83-0372,* Sandia Natl. Lab., Albuquerque, N. M.

Johnstone, J. K., G. R. Hadley, and D. R. Waymire (1985), *In situ tuff water migration/heater experiment. Final report. Rep. SAND81-1918,* Sandia Natl. Lab., Albuquerque, N. M.

Jung, J., and E. E. Ryder (1993), Thermal-mechanical analyses for the Yucca Mountain Project, in *Proceedings of the 34th US Rock Mechanics Symposium,* edited by B.C. Haimson, University of Wisconsin, Madison, June 28 to 30.

Kicker, D., M. Board, J. Leem, and M. Lin (2004), *Drift Degradation Analysis*, *ANL-EBS-MD-000027 Rev 03*. Bechtel SAIC. Las Vegas NV.

Langkopf, B. S., and P. R. Gnirk (1986), *Rock-Mass Classification of the Candidate Repository Units at Yucca Mountain, Nye County, Nevada. Rep. SAND82-2034,* Sandia Natl. Lab., Albuquerque, N. M.

Lappin, A. R. (1980), *Preliminary Thermal Expansion Screening Data for Tuffs, Rep. SAND78-1147,* Sandia Natl. Lab., Albuquerque, N. M.

Leem, J., M. Lin, Y. Sun, D. C. Kicker, and B. Damjanac (2005), Thermal-hydrologic-mechanical study of pre-closure off-normal thermal scenarios at the proposed Yucca Mountain nuclear waste reposit`ory, in *Proceedings of the 40th U.S. Rock Mechanics Symposium,* Anchorage, Alaska, June 25 to 29.

Lin, M., M. P. Hardy, and S. J. Bauer (1993), *Rock Mass Mechanical Property Estimations for the Yucca Mountain Site Characterization Project*, *Rep. SAND92-0450,* Sandia Natl. Lab., Albuquerque, N. M.

Lin, W., S. C. Blair, D. Wilder, S. Carlson, J. Wagoner, L. DeLoach, G. Danko, A. L. Ramirez, and K. Lee (2001), *Large Block Test Final Report, Tech. Rep. UCRL-ID-132246-REV-2.* Lawrence Livermore Natl. Lab., Livermore, Calif.

Lin, M., D. Kicker, B. Damjanac, M. Board, and M. Karakouzia (2007), Mechanical degradation of emplacement drifts at Yucca Mountain—a modeling case study. Part I: Nonlithophysal rock, *Int. J. Rock Mech. Min. Sci.*, *44*, 351-367.

Lin, W. N., and W. Daily (1990), Hydrological properties of Topopah spring tuff under a thermal-gradient-laboratory results, *Int. J. Rock Mech. Min. Sci. Geomech. Abstr*., *27*, 373–386.

Liu, H.-H., and J. Rutqvist (2010) A new coal-permeability model: Internal swelling stress and fracture-matrix interaction. *Transport in Porous Media*, *82*, 157-171.

Liu, H. H., and J Rutqvist (2012) Coupled hydro-mechanical processes associated with multiphase flow in a dual-continuum system: Formulations and a sensitivity study. *Rock Mechanics and Rock Engineering*, (accepted April, 2012).

Liu, H.H., J. Rutqvist, and J.C. Berryman (2009) On the relationship between stress and elastic strain for porous and fractured rock. *Int. J. Rock. Mech. Min. Sci.*, *46*, 289–296.

Liu, H.H., J. Rutqvist and J.T. Birkholzer (2011) Constitutive Relationships for Elastic Deformation of Clay Rock: Data Analysis. *Rock Mechanics and Rock Engineering*, *44*, 463–468.

Ma, L., and J. J. K. Daemen (2006), Strain rate dependent strength and stress–strain characteristics of a welded tuff, *Bull Eng Geol Env*, *65*, 221–230.

Mack, M. G., T. Brandshaug, and B. H. Brady (1989), *Rock Mass Modification Around a Nuclear Waste Repository in Welded Tuff, Tech. Rep. NUREG/CR-5390,* U.S. Nuclear Regulatory Commission, Washington, D.C.

Maerz, N. H., and W. Zhou (2005), Multivariable clustering analysis of the ECRB cross-drift discontinuities, Yucca Mountain Project, in *Proceedings of the 40th U.S. Rock Mechanics Symposium,* Anchorage, Alaska, June 25 to 29.

Manteufel, R. D., M. P. Ahola, D. R. Turner, and A. H. Chowdhury (1993), *A Literature Review of Thermal-hydrologic-mechanical-chemical Processes Pertinent to the Proposed High-level Nuclear Waste Repository at Yucca Mountain, Tech. Rep. NUREG/CR-6021*, U.S. Regulatory Commission, Washington D.C.

Martin, R. J., R. H. Price, P. J. Boyd, and J. S. Noel (1993), The influence of strain rate and sample inhomgoeneity on the moduli and strength of welded tuff. *Int. J. Rock Mech. Min. Sci. Geomech. Abstr*., 30, 1507–1510.

Martin, R. J., J. S. Noel, P. J. Boyd, and R. H. Price (1996), Thermal expansion as a function of confining pressure for welded tuff from Yucca Mountain, in *Proc. 2nd North Am. Rock Mech. Symp.*, edited by M. Aubertin, F. Hassani, Metri H., Montreal, Quebec, June 19 to 21.

Martin, R. J., J. S. Noel, P. J. Boyd, and R. H. Price (1997), Creep and static fatigue of welded tuff from Yucca Mountain, Nevada. *Int. J. Rock Mech. Min. Sci., 34*(3-4), paper No. 190.

Melo, A., and D. K. Parrish (1984), *Unit Evaluation at Yucca Mountain, Nevada Test Site: Near Field Thermal Rock Mechanics Analysis, Rep. SAND83-9939,* Sandia Natl. Lab., Albuquerque, N. M.

Min, K.-B., J. Rutqvist, and D. Elsworth (2009) Chemically and mechanically mediated influences on the transport and mechanical characteristics of rock fractures. *Int. J. Rock. Mech. Min. Sci.*, *46*, 80–89.

Mongano, G. S., W. L. Singleton, T. C. Moyer, S. C. Beason, G. L. W. Eatman, A. L. Albin, and R. C. Lung (1999), Geology *of the ECRB Cross Drift – Exploratory Studies Facility, Yucca Mountain Project, Yucca Mountain, Nevada.* Report by the U.S. Bureau of Reclamation and U.S. Geological Survey to the U.S. Department of Energy. U.S. Geological Survey, Denver, Colorado.

Morrow, C., and J. Byeflee (1984), Frictional sliding and fracture behavior of some Nevada Test Site Tuffs, in *Proceedings of the 25th US Rock Mechanics Symposium,* edited by C.H. Dowding, and M.M., Evanston, Illinois, June 25 to 27.

Mukhopadhyay, S., and Y. W. Tsang (2002), Understanding the anomalous temperature data from the large block test at Yucca Mountain, Nevada, *Water Resour. Res*., 38(10), 1210.

Neuzil, C.E. (2003), Hydromechanical coupling in geologic processes. *Hydrogeol. J*,, *11*, 41-83.

Nieder-Westermann, G. H. (1998), *Geology of the Exploratory Studies Facility Topopah Spring Loop, Tech. Rep. BAB000000-01717-0200-00002 REV01*. CRWMS M&O (Civilian Radioactive Waste Management System Management & Operating Contractor), Las Vegas, Nevada.

Nieder-Westermann, G. H. (2000), *Fracture Geometry Analysis for the Stratigraphic Units of the Repository Host Horizon. Tech Rep.* ANL-EBS-GE-000006 Rev 00. CRWMS M&O (Civilian Radioactive Waste Management System Management & Operating Contractor), Las Vegas, Nevada.

Nimick, F. B. (1988), Empirical relationships between porosity and the mechanical properties of tuff, in *Proceedings of the 29th US Symposium on Rock Mechanics*, edited by P.A. Cundall, R.L. Sterling, A.M. Starfield, University of Minnesota, June 13 to 15.

Nimick, F. B. (1989), *Thermal Conductivity Data from the Unsaturated Tuff at Yucca Mountain, Nevada, Rep. SAND88-0624*, Sandia Natl. Lab., Albuquerque, N. M.

Nitao, J. J. (1998), *User's Manual for the USNT Module of the NUFT code, Version 2.0 (NP-phase, NC-component, thermal), Tech. Rep. UCRL-MA-130653*, Lawrence Livermore Natl. Lab., Livermore, Calif.

Olsson, W. A. (1987), *Rock Joint Compliance Studies, Rep. SAND86-0177*, Sandia Natl. Lab., Albuquerque, N. M.

Olsson, W. A. (1988), *Compliance and Strength of Artificial Joints in Topopah Spring Tuff, Rep. SAND88-0660*, Sandia Natl. Lab., Albuquerque, N. M.

Olsson, W. A., and S. Brown (1995), *Mechanical properties of fractures from drill holes UE25-NRG-4, USW-NRG-6, USW-NRG-7, and USW-SD-9 at Yucca Mountain, Nevada, Rep. SAND95-1736*, Sandia Natl. Lab., Albuquerque, N. M.

Ortiz, T. S., R. K. Williams, F. B. Nimick, B. C. Whittet, and D. L. South D.L. (1985), *A Three-Dimensional Model of Reference Thermal/Mechanical and Hydrological Stratigraphy at Yucca Mountain, Southern Nevada, Rep. SAND84-1076*, Sandia Natl. Lab., Albuquerque, N. M.

Pruess, K., and J. S. Y. Wang (1984), TOUGH – a numerical model for nonisothermal unsaturated flow to study waste canister heating effects, in *Scientific Basis for Nuclear Waste Management XIX*, edited by G. L. McVay.

Pruess, K., C. Oldenburg, and G. Moridis (1999), *TOUGH2 User's Guide, Version 2.0, Rep. LBNL-43134*, Lawrence Berkeley Natl. Lab., Berkeley, Calif.

Peters, R. R., E. A. Klavetter, I. J. Hall, S. C. Blair, P. R. Heller, and G. W. Gee (1984), *Fracture and Matrix Hydrologic Characteristics of Tuffaceous Materials from Yucca Mountain, Nye County, Nevada, Rep. SAND84-1471*, Sandia Natl. Lab., Albuquerque, N. M.

Price, R. H. (1983), *Analysis of the Rock Mechanics Properties of Volcanic Tuff Units from Yucca Mountain, Nevada Test Site, Rep. SAND82-1315*, Sandia Natl. Lab., Albuquerque, N. M.

Price, R. H. (2004), *The Mechanical Properties of Lithophysal Tuff: Laboratory Experiments, YMP Project Report TDR-EBS-MD-000027 Rev 00*, Department of Energy, Yucca Mountain Project, Las Vegas, N. V.

Price, R. H., and S. J. Bauer (1985), Analysis of the elastic and strength properties of Yucca Mountain tuff, Nevada, in *Proceedings of the 26th US Symposium on Rock Mechanics*, edited by E. Ashworth, Rapid City, S. D, June 26 to 28.

Price, R. H., R. J. Martin III, and P. J. Boyd (1993), Characterization of porosity in support of mechanical property analysis. in *Proceedings of the 4th International Conference on High Level Radioactive Waste Management Conference*, Las Vegas, Nevada.

Price, R. H., R. J. Martin III R.J., Boyd P.J., and Noel J.S. (1994), Mechanical and bulk properties in support of ESF design issues. in *Proceedings of the 5th International Conference on High Level Radioactive Waste Management Conference*, Las Vegas, Nevada.

Rinaldi, A.P., J. Rutqvist, E. L. Sonnenthal (2012) TOUGH-FLAC coupled THM modeling of proposed stimulation at the Newberry volcano EGS demonstration. Proceedings, TOUGH Symposium 2009, Lawrence Berkeley National Laboratory, Berkeley, California, September 17-19, 2012.

Rutqvist, J. (2004), *Drift-Scale THM Model Report, Tech. Rep. MDL-NBS-HS-000017 rev 01*. Bechtel SAIC, Las Vegas, N. V.

Rutqvist, J. (2009), Estimating stress-versus-permeability relationships of fractured rock using data from in situ experiments and effects of chemical-mechanical coupling, in *Proceedings of the International Conference on Rock Joints and Jointed Rock Masses*, Tucson, Arizona, Jan 4 to 10.

Rutqvist, J. (2011), Status of the TOUGH-FLAC simulator and recent applications related to coupled fluid flow and crustal deformations. *Comput. Geosci.*, *37*, 739–750.

Rutqvist J. (2012), The geomechanics of CO_2 storage in deep sedimentary formations. *International Journal of Geotechnical and Geological Engineering, 30*, 525–551.

Rutqvist J. and G.J. Moridis G.J. (2009), Numerical Studies on the Geomechanical Stability of Hydrate-Bearing Sediments. Society of Petroleum Engineers, SPE-126129, *SPE Journal*, *14*, 267–282.

Rutqvist J. and O. Stephansson (2003), The role of hydromechanical coupling in fractured rock engineering. *Hydrogeol. J, 11*, 7–40.

Rutqvist, J., and C.- F. Tsang (2003), Analysis of thermal-hydrologic-mechanical behavior near an emplacement drift at Yucca Mountain, *J. Contam. Hydr*ol., *62–63*, 637–652.

Rutqvist J., L. Börgesson, M. Chijimatsu, A. Kobayashi, T. S. Nguyen, L. Jing, J. Noorishad, and C.-F. Tsang (2001a), Thermohydromechanics of partially saturated geological media – Governing equations and formulation of four finite element models. *Int. J. Rock Mech. Min. Sci., 38*, 105–127.

Rutqvist, J., L. Börgesson, M. Chijimatsu, T.S. Nguyen, L. Jing, J. Noorishad, and C.-F. Tsang (2001b), Coupled Thermo-hydro-mechanical Analysis of a Heater Test in Fractured Rock and Bentonite at Kamaishi Mine – Comparison of Field Results to Predictions of Four Finite Element Codes. *Int. J. Rock Mech. Min. Sci. 38*, 129–142.

Rutqvist, J., Y. S. Wu, C.- F. Tsang, and G. Bodvarsson (2002), A Modeling Approach for Analysis of Coupled Multiphase Fluid Flow, Heat Transfer, and Deformation in Fractured Porous Rock, *Int. J. Rock Mech. Min. Sci.*, *39*, 429–442.

Rutqvist, J., D. Barr, R. Datta, A. Gens, M. Millard, S. Olivella, C.- F. Tsang, and Y. Tsang (2005), Coupled thermal-hydrological-mechanical analysis of the Yucca Mountain Drift Scale Test – comparison of field results to predictions of four different models, *Int. J. Rock Mech. Min. Sci*., *42*, 680–697.

Rutqvist, J., B. Freifeld, K. -B. Min, D. Elsworth, and Y. Tsang (2008a), Analysis of thermally induced changes in fractured rock permeability during eight years of heating and cooling at the Yucca Mountain Drift Scale Test, *Int. J. Rock Mech. Min. Sci.*, *45*, 1373–1389.

Rutqvist, J., D. Barr, J. T. Birkholzer, M. Chijimatsu, O. Kolditz, Q.-S Liu, Y. Oda, W.- Q. Wang, and C. Y. Zhang (2008b), Results from an international simulation study on coupled thermal, hydrological, and mechanical (THM) processes near geological nuclear waste repositories, *Nucl. Technol.*, *163*, 101–109.

Rutqvist, J., D. Barr, J. T. Birkholzer, K. Fujisaki, O. Kolditz, Q. -S. Liu, T. Fujita, W. Wang, and C. -Y Zhang (2009), A comparative simulation study of coupled THM processes and their effect on fractured rock permeability around nuclear waste repositories, *Environ. Geol.*, *57*, 1347–1360.

Rutqvist, J., G.J. Moridis, T. Grover, and T. Collett (2009) Geomechanical response of permafrost-associated hydrate deposits to depressurization-induced gas production. *J. Petrol. Sci. Eng.*, *67*, 1–12.

Rutqvist, J., D. Vasco, and L. Myer. (2010a) Coupled reservoir-geomechanical analysis of CO2 injection and ground deformations at In Salah, Algeria. *Int. J. Greenhouse Gas Control*, *4*, 225–230.

Rutqvist, J., C.M. Oldenburg, P.F. Dobson, J. Garcia, and M. Walters (2010b) Predicting the spatial extent of injection-induced zones of enhanced permeability at the Northwest Geysers EGS demonstration project. Proceedings of the 44th U.S. Rock Mechanics Symposium, Salt Lake City, Utah, USA, June 27-June 30, 2010: American Rock Mechanics Association ARMA, Paper No. 502.

Rutqvist, J., Y. Ijiri, and H. Yamamoto (2011) Implementation of the Barcelona Basic Model into TOUGH-FLAC for simulations of the geomechanical behavior of unsaturated soils. *Comput. Geosci.*, *37*, 751–762.

Rutqvist, J., H.-M. Kim, D.-W. Ryu, J.-H. Synn, and W.-K. (2012) Song Modeling of coupled thermodynamic and geomechanical performance of underground compressed air energy storage in lined rock caverns. *Int. J. Rock. Mech. Min. Sci.*, *52*, 71–81.

Schwartz, B., and C. S. Chocas (1992), Linear Thermal Expansion Data for Tuffs from the Unsaturated Zone at Yucca Mountain, Nevada, *Rep. SAND88-1581*. Sandia Natl. Lab., Albuquerque, N. M.

Smith, S., and R. Snieder (2010), Seismic modeling and analysis of a prototype heated nuclear waste storage tunnel, Yucca Mountain, Nevada, *Geophysics*, *75*, T1–T8.

Sobolik, S. R., R. E. Finley, and S. Ballard (1998), Post-Test Comparison of Thermal Mechanical Measurements vs. Analyses for the In-Situ Single Heater Test, Yucca Mountain, Nevada, *Int. J. Rock Mech. Min. Sci.*, *35*(4-5) Paper no. 659.

Sobolik, S. R., R. E. Finley, and S. Ballard (1999), Thermal-Mechanical Measurements in the Drift Scale Test, Yucca Mountain, Nevada, in *Proceedings of the 37th US Rock Mechanics Symposium*, edited by B. Amadei B, R. L. Kranz RL, G. A. Scott and P. H. Smeallie PH, Vail, Colorado, June 6 to 9.

Sonnenthal, E., A. Ito, N. Spycher, M. Yui, J. Apps, Y. Sugita, M. Conrad, and S. Kawakami (2005), Approaches to modeling coupled thermal, hydrological, and chemical processes in the drift scale heater test at Yucca Mountain, Int. J. Rock Mech. Min. Sci., 42, 698–719

Spycher, N. F., E. L. Sonnenthal, and J. A. Apps (2003), Fluid flow and reactive transport around potential nuclear waste emplacement tunnels at Yucca Mountain, Nevada, *J. Contam. Hydrol., 62–63*, 653–673.

Sun, Y., F. Fuan, M. Lin, and N. Doraswami (2001), *Ground Control for Emplacement Drifts for SR, Tech. Rep. ANL-EBS-GE-000002 Rev 00 ICN01*. Bechtel SAIC. Las Vegas N. V.

Sun, Y. (2001), Prediction of long-term stability of emplacement drifts at Yucca Mountain, in *Proceedings of the 38th US Rock Mechanics Symposium*, edited by D. Elsworth, J. P. Tinucci, and K. A. Heasley, Washington D.C., July 7 to 10.

Sweetkind, D. S., S. C. Williams-Stroud, and J. A. Coe (1997), *Characteristics of the Fracture Network at Yucca Mountain, Nevada: Part 1. Integration of Field Data for Numerical Simulations*, in *Fractured reservoirs: Characterization and Modeling*, edited by T. E. Hoak, A. L. Klavitter, P. K. Blomquist, Rocky Mountain Association of Geologists, Denver, Colorado.

Todesco, M., J. Rutqvist, G. Chiodini, K. Pruess, and C.M. Oldenburg (2004) Modeling of recent volcanic episodes at Phlegrean Fields (Italy): geochemical variations and ground deformation. Geothermics, *33*, 531–547.

Tolefson, J. (2011), Battle of Yucca Mountain Rages on, *Nature*, *473*, 266-267.

Thomas, R. K. (1984), *Unit Evaluation at Yucca Mountain, Nevada Test Site: Near Field Mechanical Calculation Using a Continuum Jointed Rock Model in the JAC code, Rep. SAND83-0070.* Sandia Natl. Lab., Albuquerque, N. M.

Tsang, C.-F. (Ed.) (1987), *Coupled Processes Associated With Nuclear Waste Repositories*, Academic, Orlando, Fla.

Tsang, C.-F. (1991), Coupled thermomechanical hydrochemical processes in rock fractures. *Rev. Geophys.*, 29, 537–551.

Tsang, C.-F. (1999), Linking thermal, hydrological and mechanical processes in fractured rocks. *Annu. Rev. Earth Planet. Sci.*, 27, 359–384.

Tsang, C-F., O. Stephansson, L. Jing, and F. Kautsky (2009a), DECOVALEX Project: from 1992 to 2007, *Environmental Geology, 57(6), 1221-1237.*

Tsang, Y. W., J. Apps, J. T. Birkholzer, B. Freifeld, M. Q. Hu, J. Peterson, E. Sonnenthal, and N. Spycher (1999), *Yucca Mountain single heater test final report, Tech. Rep. LBNL- 42537*, Lawrence Berkeley Natl. Lab., Berkeley, Calif.

Tsang, Y. W., and J. T. Birkholzer (1999), Predictions and observations of the thermal-hydrological conditions in the single heater test, *J. Contam. Hydrol., 38*, 385–425.

Tsang, Y. W., J. T. Birkholzer, and S. Mukhopadhyay (2009b), Modeling of thermally driven hydrological processes in partially saturated fractured rock, *Rev. Geophys., 47*, RG3004

Tyler, L. D. (1980), Thermal/mechanical modeling for a tuff repository, in *Proceedings of Workshop on Thermalmechanical-hydrochemical Modeling for a Hardrock Waste Repository*, Berkeley, California, July 29 to 31, *Rep. LBL-11204*, Lawrence Berkeley Natl. Lab, Berkeley, Calif.

Wagner, R. (2002), *Thermal Testing Measurements Report. ANL-NBS-HS-000041 REV 00.* Las Vegas, Nevada: Bechtel SAIC Company.

Wang, J., and P. Cook (2005), Air-permeability distributions at niches in tuff units at Yucca Mountain, in *Proceedings of the 40th U.S. Rock Mechanics Symposium*, Anchorage, Alaska, June 25 to 29.

Wang, J. S. Y., and D. Elsworth (1999), Permeability changes induced by excavation in fractured tuff. in *Proceedings of the 37th US Rock Mechanics Symposium*, edited by B. Amadei B, R. L. Kranz RL, G. A. Scott and P. H. Smeallie PH, Vail, Colorado, June 6 to 9.

Wang, J. S. Y., and G.S. Bodvarsson (2003), Evolution of the unsaturated zone testing at Yucca Mountain. *J. Contam. Hydrol., 62-63*, 337–360.

Wang, J., P. Cook, R. Trautz, S. Flexser, Q. Hu, R. Salve, D. Hudson, M. Conrad, Y. Tsang , K. Williams, W. Sol, and J. Turin (2001), *In-situ field testing of processes, Rep. ANL-NBS-HS-000005 REV01*. Las Vegas, Nevada: Bechtel SAIC Company.

Wang, W., J. Rutqvist, U.-J. Görke, J.T. Birkholzer, and O. Kolditz (2011) Non isothermal flow in low permeable porous media: A comparison of Richards' and two-phase flow approaches. *Environmental Earth Sciences*, *62*, 1197–1207.

Yasuhara, H., D. Elsworth, and A. Polak (2004), Evolution of permeability in a natural fracture: significant role of pressure solution. *J. Geophys. Res.*, *109*, B3204.

Zimmerman, R. M. (1982), Issues related to field testing in tuff. in *Proceedings of the 23rd US Rock Mechanics Symposium*, edited by R. E. Goodman and F. Heuze, Berkeley, California, August 25 to 27.

Zimmerman, R. M., M. P. Board, E. H. Hardin, and M. D. Voegele (1984), Ambient temperature testsing of the G-Tunnel Heated Block, in Proceedings of the 25th US Symposium on Rock Mechanics, edited by C.H. Dowding, and M.M., Evanston, Illinois, June 25 to 27.

Zimmerman, R. M., M. L. Wilson, M. P. Board, M. E. Hall, and R. L. Schuch (1985), Thermal-Cycle Testing of the G-Tunnel Heated Block, in Proceedings of the 26th US Symposium on Rock Mechanics, edited by E. Ashworth, Rapid City, S. D, June 26 to 28.

Zimmerman, R. M., M. L. Blanford, J. F. Holland, R. L. Schuch, and W. H. Barrertt (1986a), *Final report: G-Tunnel small-diameter heater experiments, Rep. SAND84-2621*, Sandia Natl. Lab., Albuquerque, N. M.

Zimmerman, R. M., R. L. Schuch, D. S. Mason, M. L. Wilson, M. E. Hall, M. P. Board, R. P. Bellman, and M. L. Blanford (1986b), *Final report: G-Tunnel heated block experiments*, *Rep. SAND84-2620*, Sandia Natl. Lab., Albuquerque, N. M.

Zimmerman, R. M., K. L. Mann, and D. J. Dodds (1989), Results of pressurized-slot measurements in the G-Tunnel underground facility. in *Proceedings of the 30th US Rock Mechanics Symposium*, edited by A.W. Khair, West Virginia University, Morgantown, June 19 to 22.

Zoback, M.D. (2007), Reservoir geomechanics. Cambridge University Press, Cambridge

FIGURE CAPTIONS

Figure 1. (a) The Yucca Mountain at the Nevada Test Site, Nevada, and (b) vertical cross section of Yucca Mountain showing lithostratigraphic units and the then proposed repository horizon in the unsaturated zone (modified from Wang and Bodvarsson, [2003]).

Figure 2. Short-term thermally driven coupled processes (left) and potential long-term changes around an emplacement tunnel (right).

Figure 3. Horizontal geologic cross-section of the Yucca Mountain showing underground facilities for the site investigation and the previously proposed repository outline (modified from Wang and Bodvarsson, [2003]).

Figure 4. Three classical geomechanical laboratory test results from the Yucca Mountain project related to strength and deformability of Yucca Mountain welded tuff: (a) Young's modulus and (b) ultimate compressive strength as a function of porosity and (c) ultimate compressive strength as function of sample size (modified from Price et al., 1993]).

Figure 5. (left) Photo of the sidewall of the ESF showing welded tuff with lithophysae in the Tptpul unit and 12-in diameter borehole drilled for large scale lithophysal sample, and (right) large lithophysal core sample (290 mm or 11.5-in diameter in uniaxial compression (Kicker et al. 2004; Rutqvist, 2004).

Figure 6. Static-fatigue data for unconfined and triaxial compression of heated, saturated, welded tuff and Lac Du Bonnet granite [Kicker et al., 2004; Damjanac et al, 2007]

Figure 7. Mean coefficient of thermal expansion for confined and unconfined tests on air-dried TSw2 specimens (error bars represents ± standard deviation) (after Brodsky et al., [1997]).

Figure 8. Various scales on which characterization data for repository were collected, (lower left) an example of a large diameter borehole in the Cross Drift wall in low quality Tptpll rock where some spalling fractures can be observed next to the tunnel wall, (lower right) setup of a pressurized slot test (modified from Costin et al., 2009).

Figure 9. Extrapolation of multi-scale rock strength data (modified from Costin et al., 2009].

Figure 10. Perspective of G-tunnel heated block experiment (modified from Zimmerman et al., [1985]).

Figure 11. Hydraulic conducting aperture as a function of normal stress evaluated from the G-tunnel in situ block experiment. The data from Zimmerman et al. [1985] are separated in

sequential steps showing additional fracture closure as a result of heating. The symbols are experimental data and the lines are fitted exponential functions.

Figure 12. Comparison of calculated and measured displacement in the E-W direction for the two thermal loading cycles. Positive displacement is expansion [Costin and Chen, 1991].

Figure 13. Schematic three-dimensional perspective of the SHT [Tsang et al., 2009] and photo of single heater test block insulated [Wang and Bodvarsson, 2003].

Figure 14. Measured (a) and pre-test predicted (b) displacement for six anchors along one subhorizontal extensometer borehole oriented normal to the heat sources [Cho, 1999].

Figure 15. Simulated fracture liquid saturation at 9 months of heating in single-heater test vertical cross section intersecting the in the middle of the heater [Tsang et al., 2009].

Figure 16. Evolution of air permeability measurements measured in packed off borehole sections at various distances from the heat source before, during and after heating phase of the SHT [Tsang et al., 2009].

Figure 17. (a) Photo of the LBT block of Topopah Spring Tuff at Fran Ridge, (b) Schematic three-dimensional perspective of the LBT showing heaters and boreholes for monitoring of displacements [Blair, 2001] and (c) mapped fractures [Lin et al. 2001].

Figure 18. Modeling results for relative displacement along WM2 (modified from Blair [2001]).

Figure 19. Pre/post-excavation permeability tests conducted in partially saturated tuff at Yucca Mountain. (a) Geometry of the tunnel and test boreholes, and (b) measured and simulated ratio of pre- and post-excavation permeability plotted against pre-excavation permeability [Rutqvist, 2004].

Figure 20. Histogram of permeability distribution derived from permeability measurements before and after excavation for (a) four niches excavated in the Tptpmn unit, and for (b) one niche excavated in the Tptpll unit [Rutqvist, 2004].

Figure 21. Three-dimensional view of the Yucca Mountain Drift Scale Test. The color-coded lines indicate boreholes for various measurements of thermally driven THMC responses [Tsang et al., 2009].

Figure 22. Calculated contours of (a) temperature, (b) change in liquid fracture saturation, (c) change in horizontal stress, and (d) permeability change factor in the NW-striking fracture set after 1 year of heating [Rutqvist et al. 2005].

Figure 23. Results of geophysical field measurement to evaluate changes in the superheated zone. The contours of ERT relative saturation and neutron water content (left) and change is matrix saturation inferred from ground-penetrating radar (middle) was extracted from Tsang et al. [2009], whereas compressional velocity contour (right) was extracted from Smith and Snieder [2010]. Dashed lines in the left and middle figure are the calculated extent of the dryout zone corresponding to the extent of the <50% matrix saturation; Note that the seismic velocity change (right) was evaluated for an assumed elliptically shaped velocity structure that was also assumed to be constant over the 4 years of heating.

Figure 24. Comparison of simulated and measured temperature, displacement, and permeability change factor [Rutqvist, 2004].

Figure 25. Ground support for emplacement drifts with steel sets and fully grouted rock bolts (top), and (bottom) calculated axial forces along rock bolts for in situ and thermal load (modified from Sun et al. [2001]).

Figure 26. Calculated rock fall after 10,000 years caused by the combined effects of in situ stress, thermal stress, and time-dependent strength degradation for a drift located in (a) Category 2 and (b) Category 5, lithophysal rock [Kicker et al., 2004, Damjanac et al., 2007]

Figure 27. Schematic of thermally driven mechanical changes around a repository tunnel [Rutqvist et al., 2009].

Figure 28. Effects of THM-induced changes in hydrological properties. (a) Effects on the extent of the dryout zone after 1000 years, and (b) effects on the liquid fluid flow pattern at 10,000 years [Rutqvist et al., 2009].

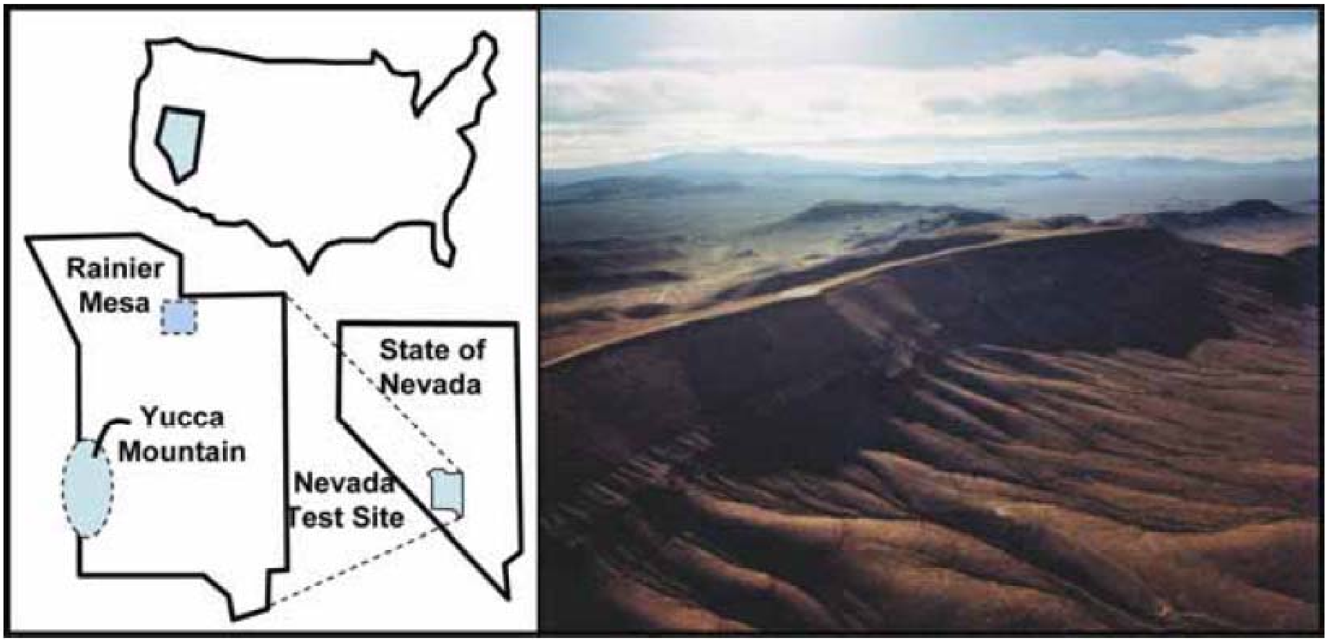

(a)

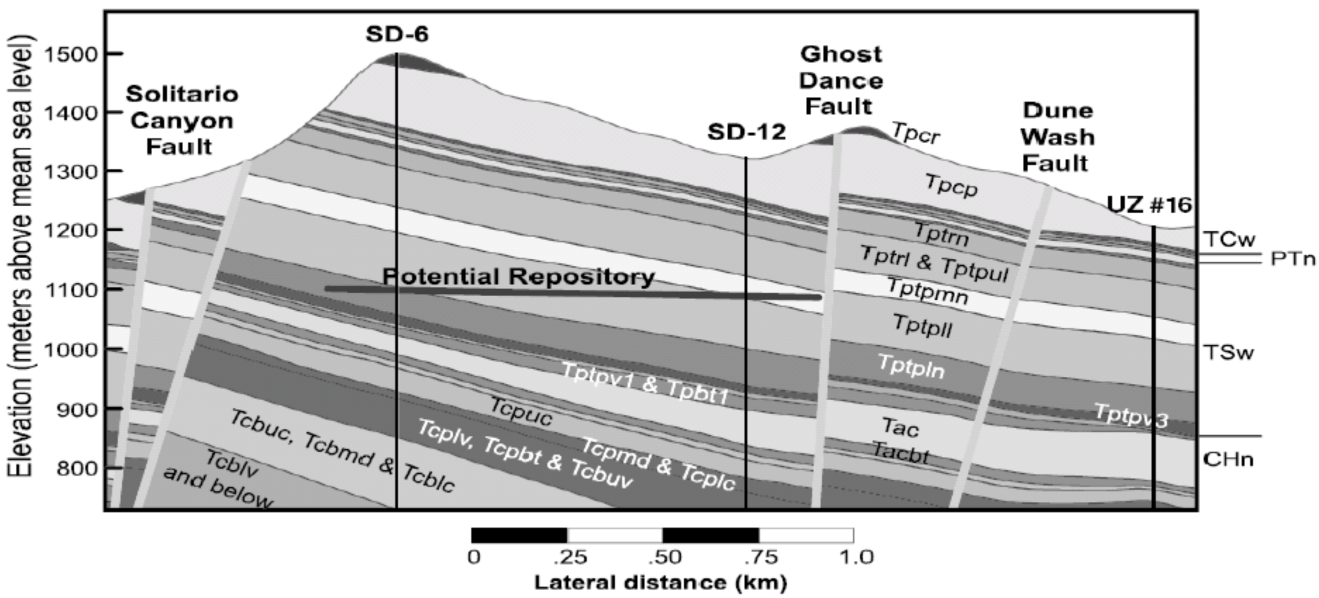

(b)

Figure 1. (a) The Yucca Mountain at the Nevada Test Site, Nevada, and (b) vertical cross section of Yucca Mountain showing lithostratigraphic units and the then proposed repository horizon in the unsaturated zone (modified from Wang and Bodvarsson, [2003]).

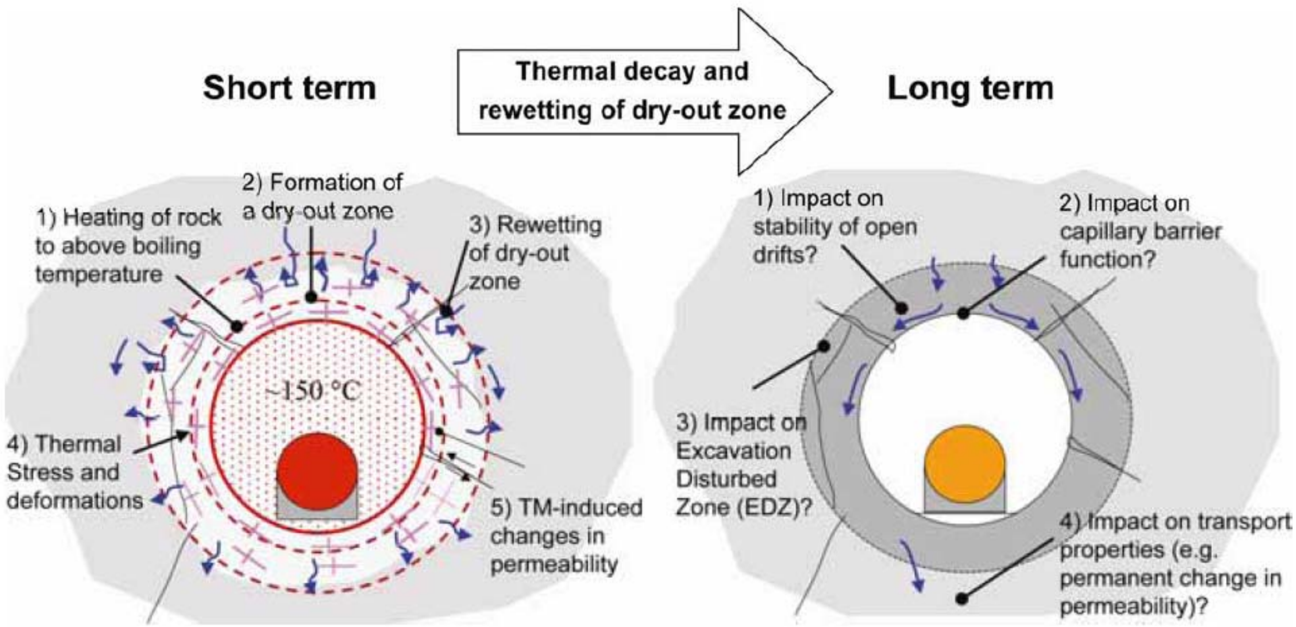

Figure 2. Short-term thermally driven coupled processes (left) and potential long-term changes around an emplacement tunnel (right).

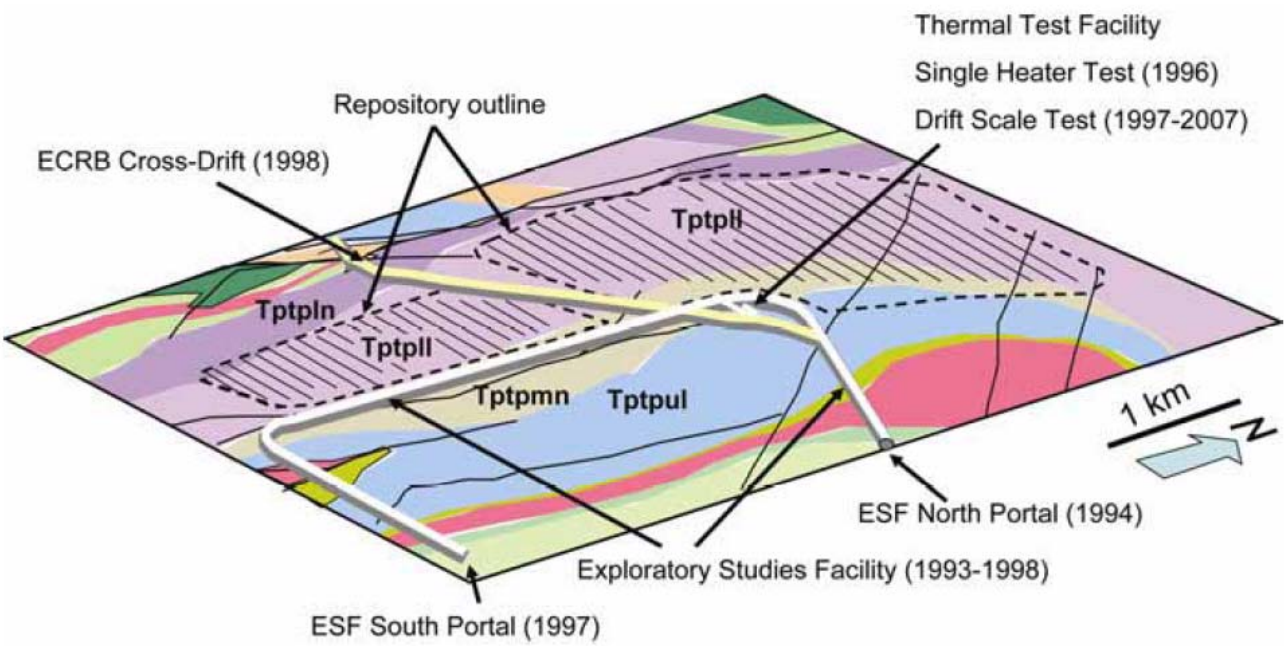

Figure 3. Horizontal geologic cross-section of the Yucca Mountain showing underground facilities for the site investigation and the previously proposed repository outline (modified from Wang and Bodvarsson, [2003]).

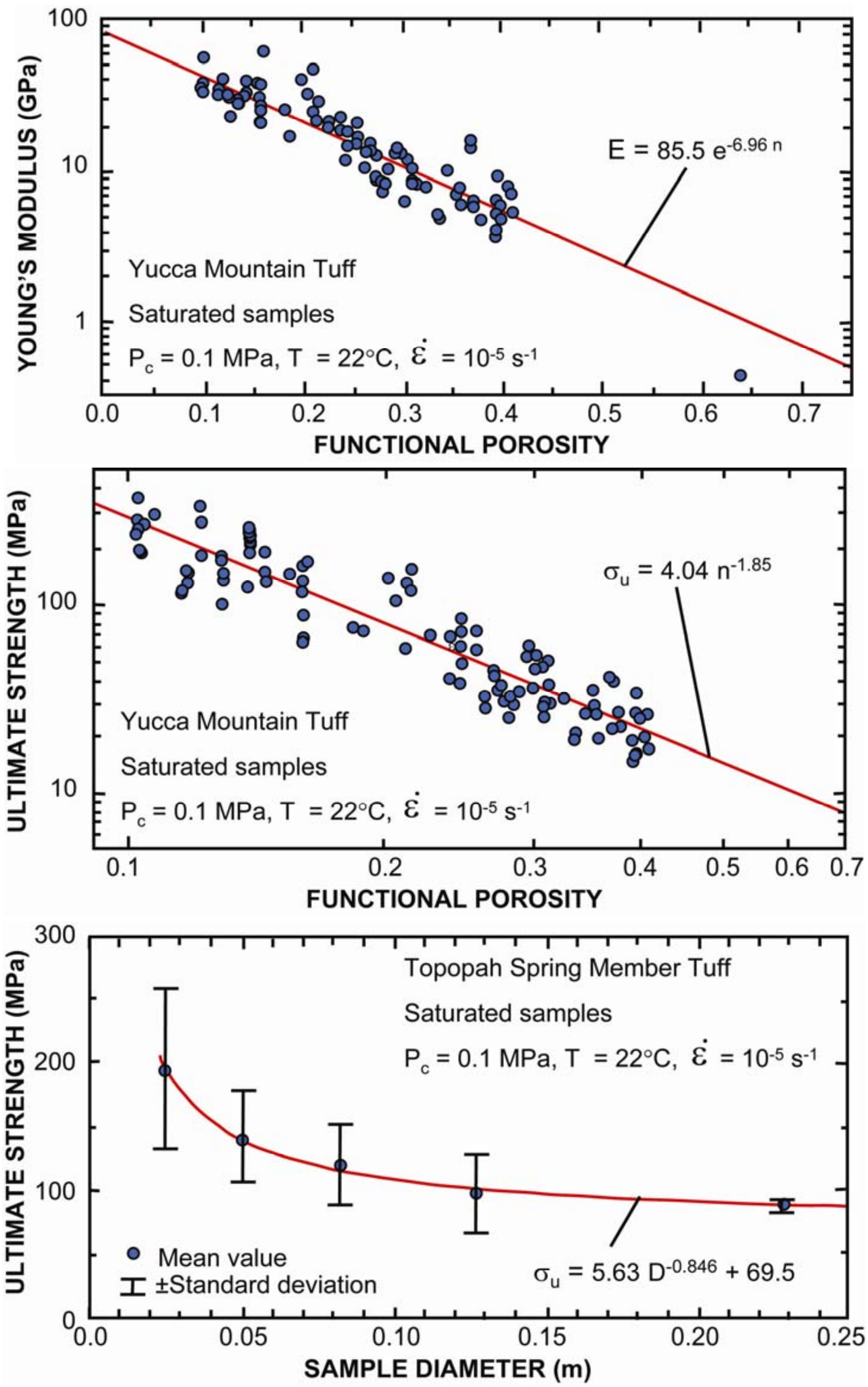

Figure 4. Three classical geomechanical laboratory test results from the Yucca Mountain project related to strength and deformability of Yucca Mountain welded tuff: (a) Young's modulus and (b) ultimate compressive strength as a function of porosity and (c) ultimate compressive strength as function of sample size (modified from Price et al., 1993]).

Figure 5. (left) Photo of the sidewall of the ESF showing welded tuff with lithophysae in the Tptpul unit and 12-in diameter borehole drilled for large scale lithophysal sample, and (right) large lithophysal core sample (290 mm or 11.5-in diameter in uniaxial compression (Kicker et al. 2004; Rutqvist, 2004).

.

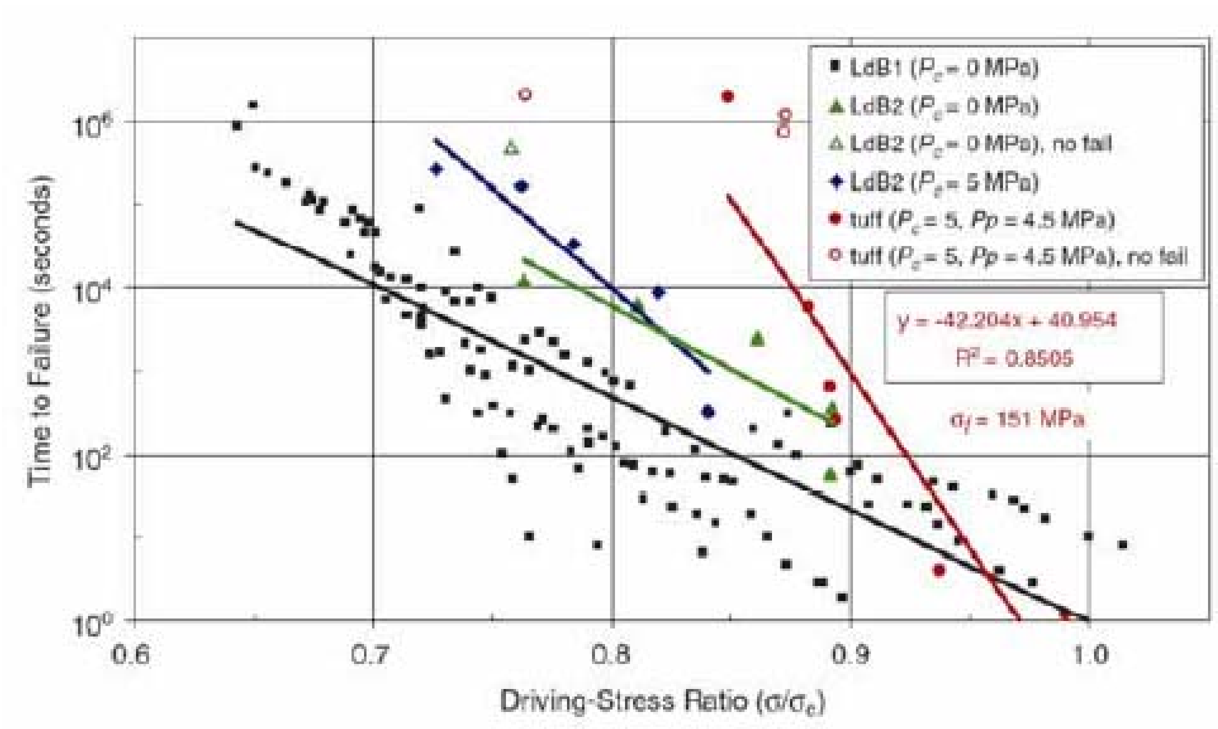

Figure 6. Static-fatigue data for unconfined and triaxial compression of heated, saturated, welded tuff and Lac Du Bonnet granite [Kicker et al., 2004; Damjanac et al, 2007]

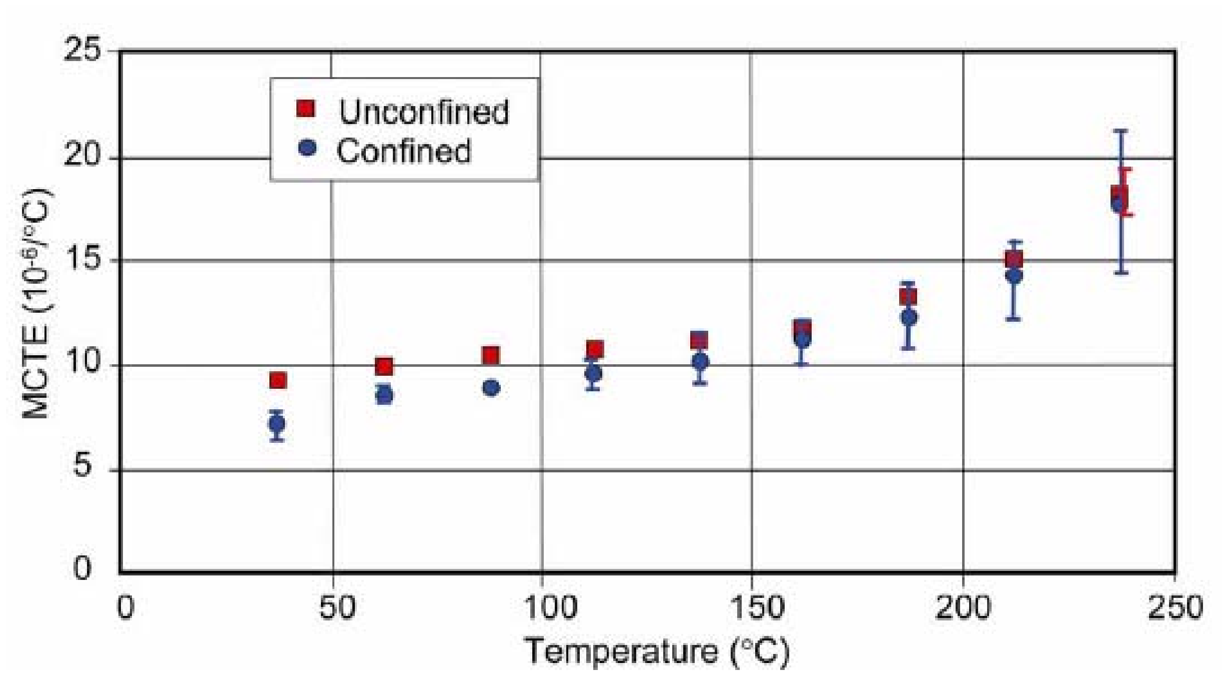

Figure 7. Mean coefficient of thermal expansion for confined and unconfined tests on air-dried TSw2 specimens (error bars represents ± standard deviation) (after Brodsky et al., [1997]).

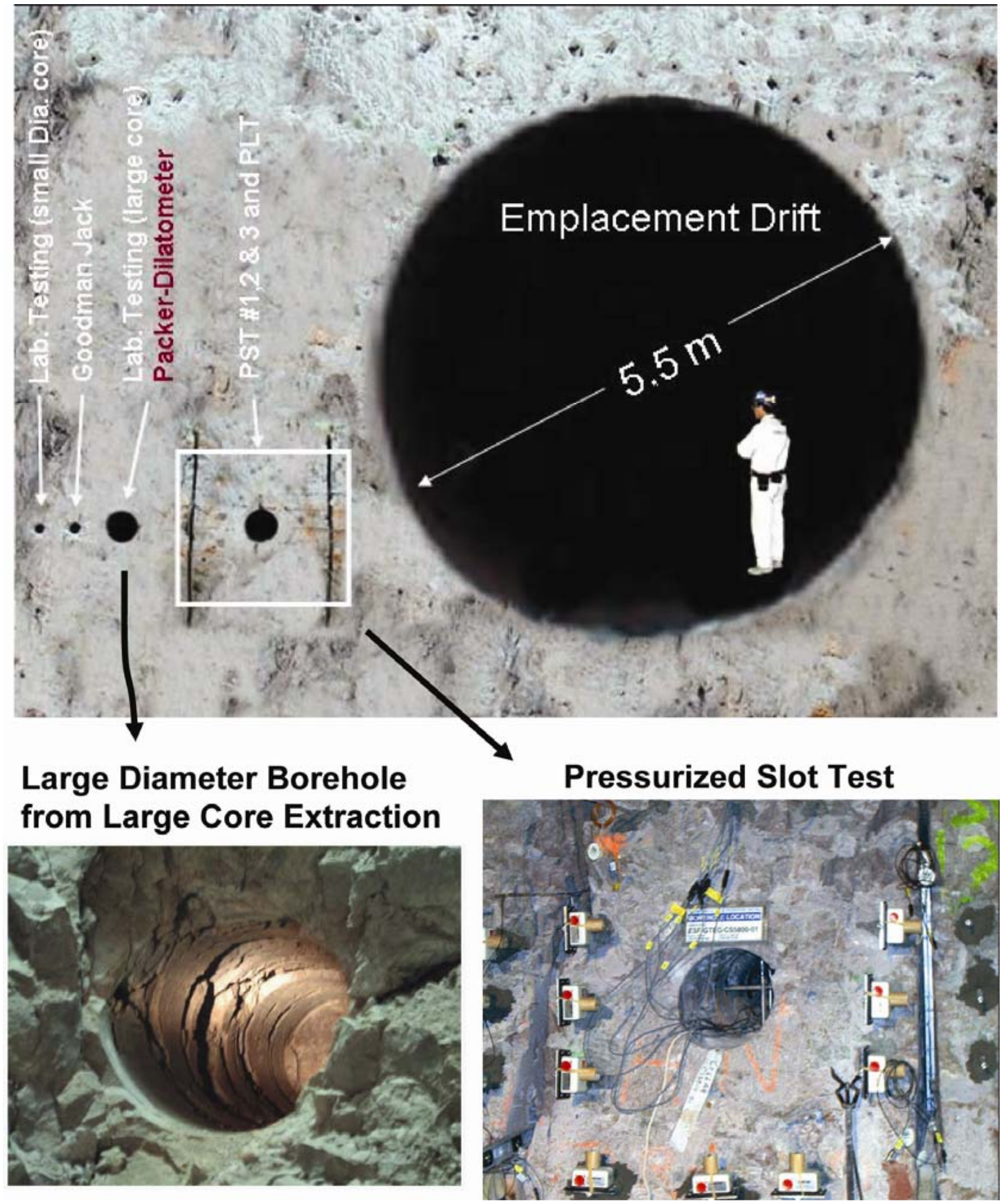

Figure 8. Various scales on which characterization data for repository were collected, (lower left) an example of a large diameter borehole in the Cross Drift wall in low quality Tptpll rock where some spalling fractures can be observed next to the tunnel wall, (lower right) setup of a pressurized slot test (modified from Costin et al., 2009).

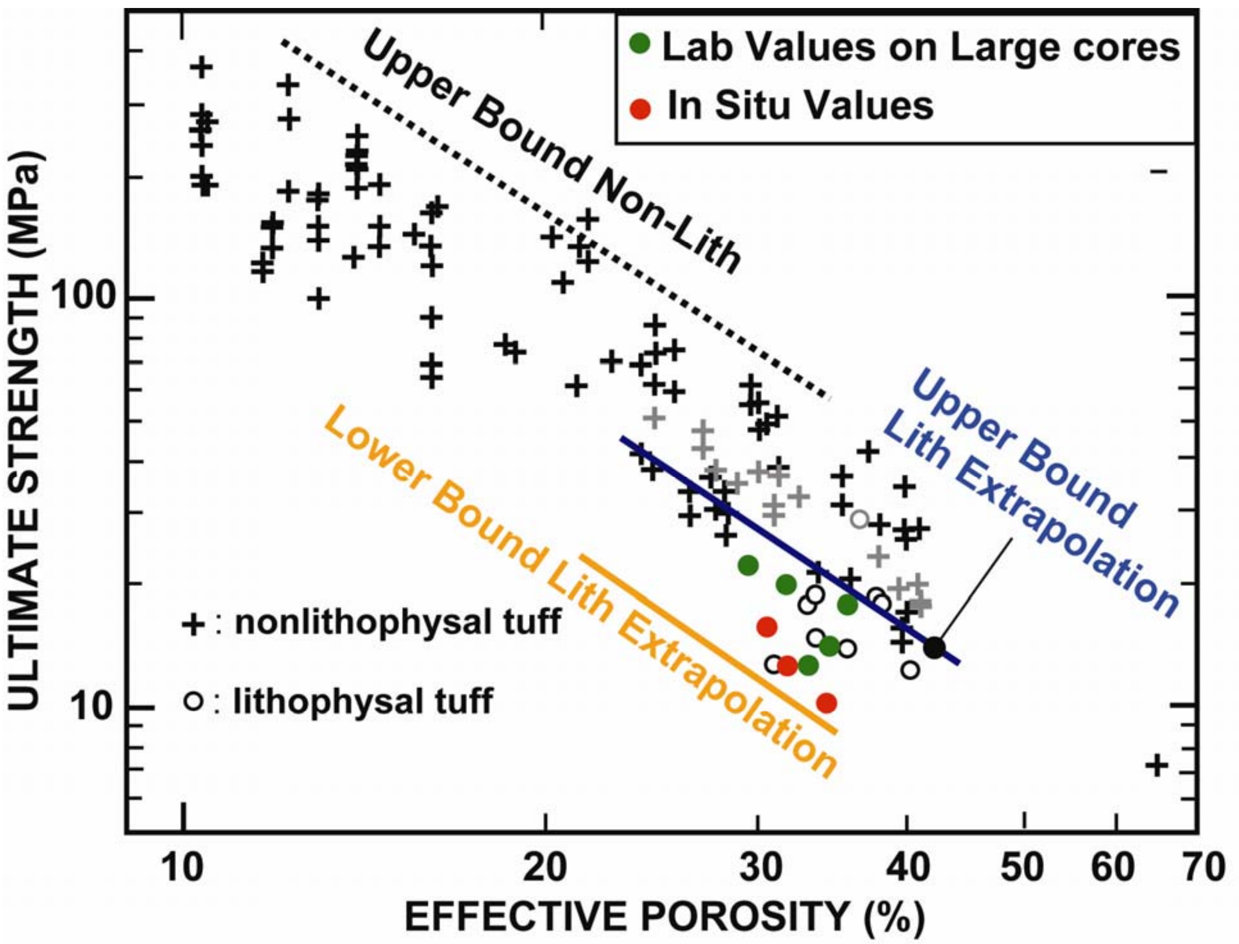

Figure 9. Extrapolation of multi-scale rock strength data (modified from Costin et al., 2009].

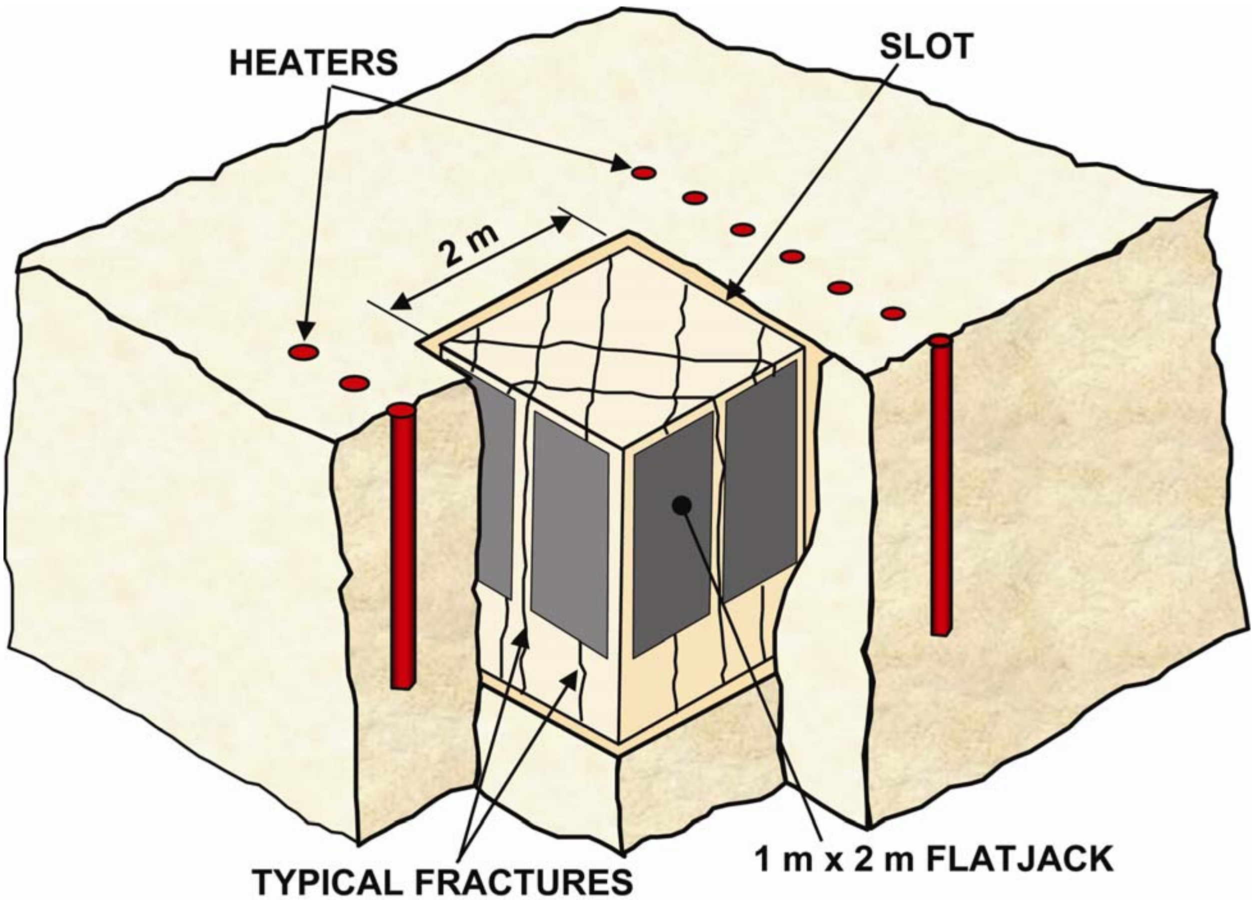

Figure 10. Perspective of G-tunnel heated block experiment (modified from Zimmerman et al., [1985]).

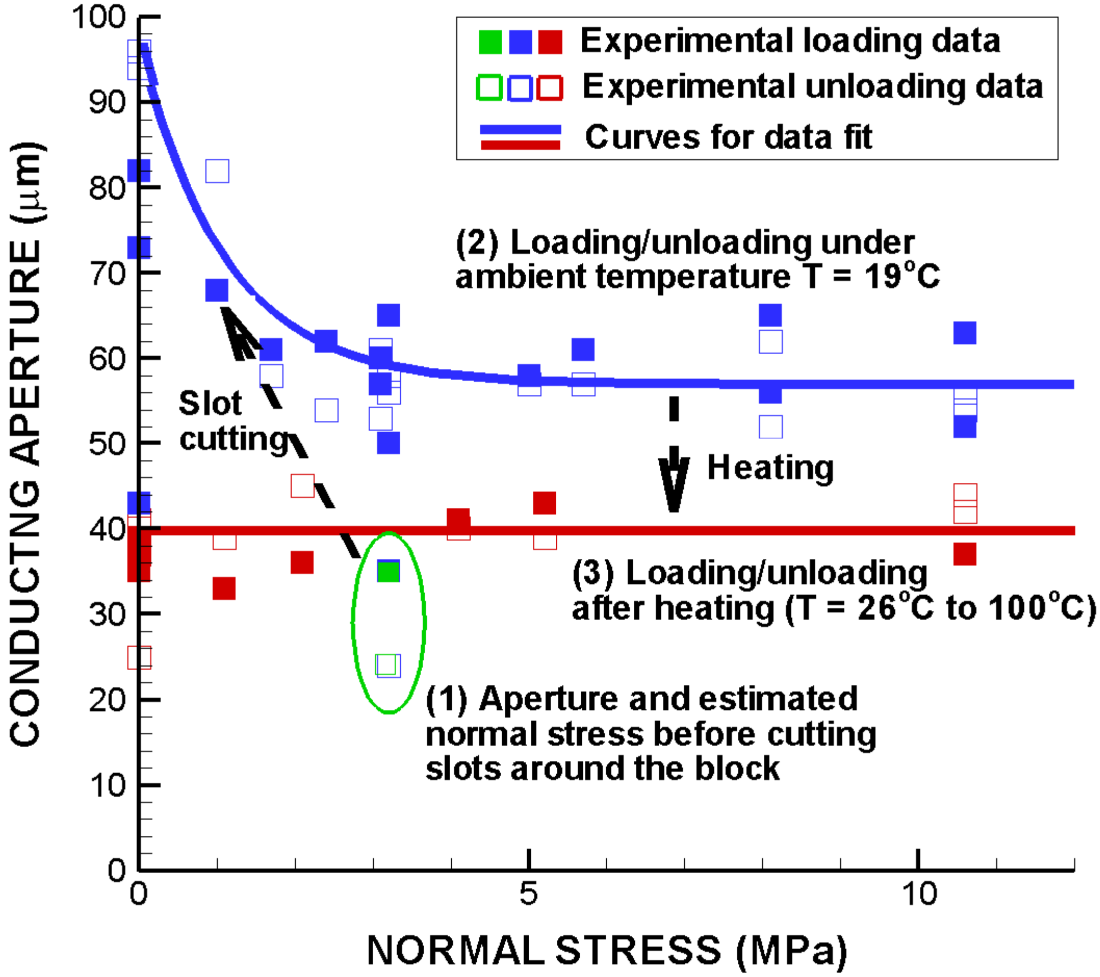

Figure 11. Hydraulic conducting aperture as a function of normal stress evaluated from the G-tunnel in situ block experiment. The data from Zimmerman et al. [1985] are separated in sequential steps showing additional fracture closure as a result of heating. The symbols are experimental data and the lines are fitted exponential functions.

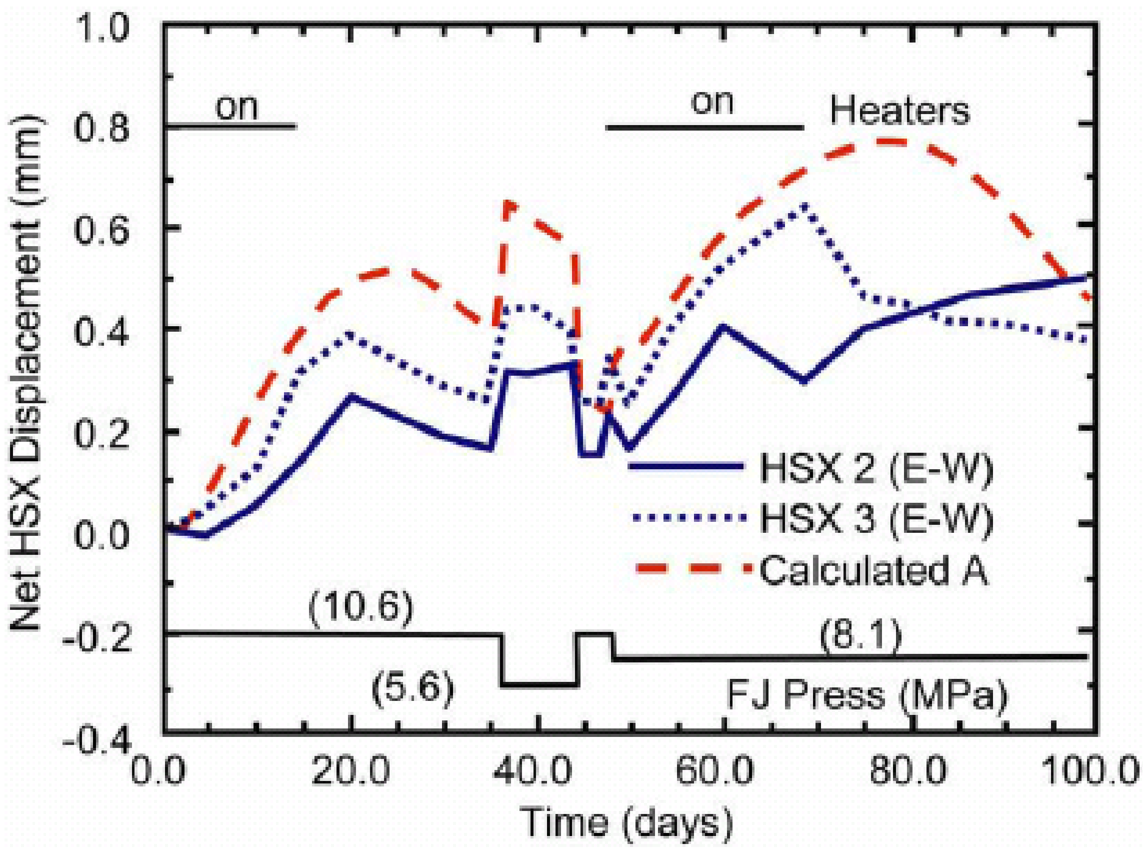

Figure 12. Comparison of calculated and measured displacement in the E-W direction for the two thermal loading cycles. Positive displacement is expansion [Costin and Chen, 1991].

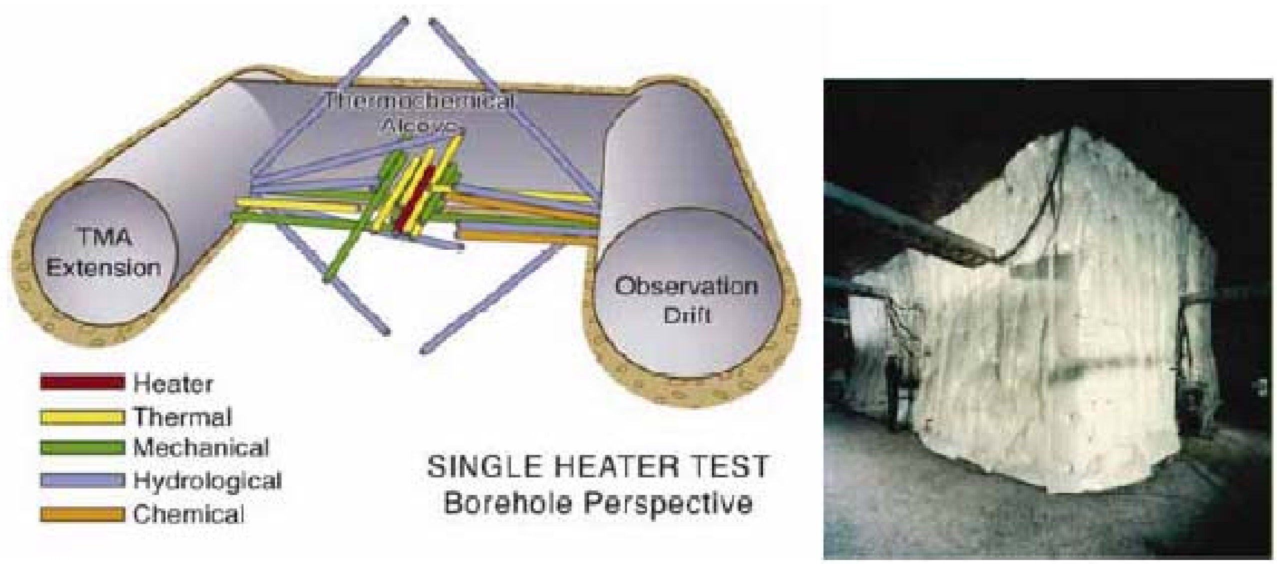

Figure 13. Schematic three-dimensional perspective of the SHT [Tsang et al., 2009] and photo of single heater test block insulated [Wang and Bodvarsson, 2003].

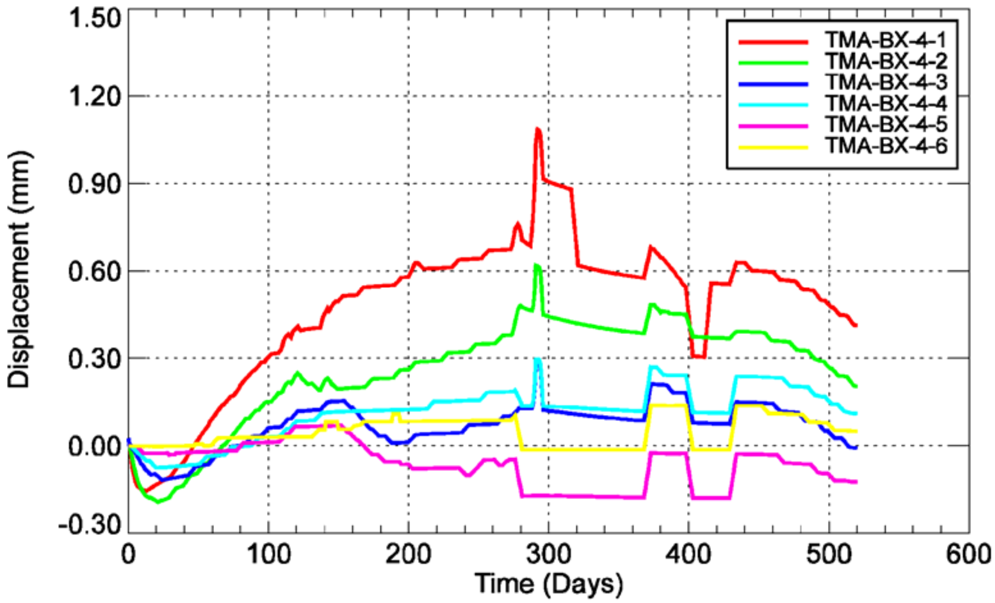

(a)

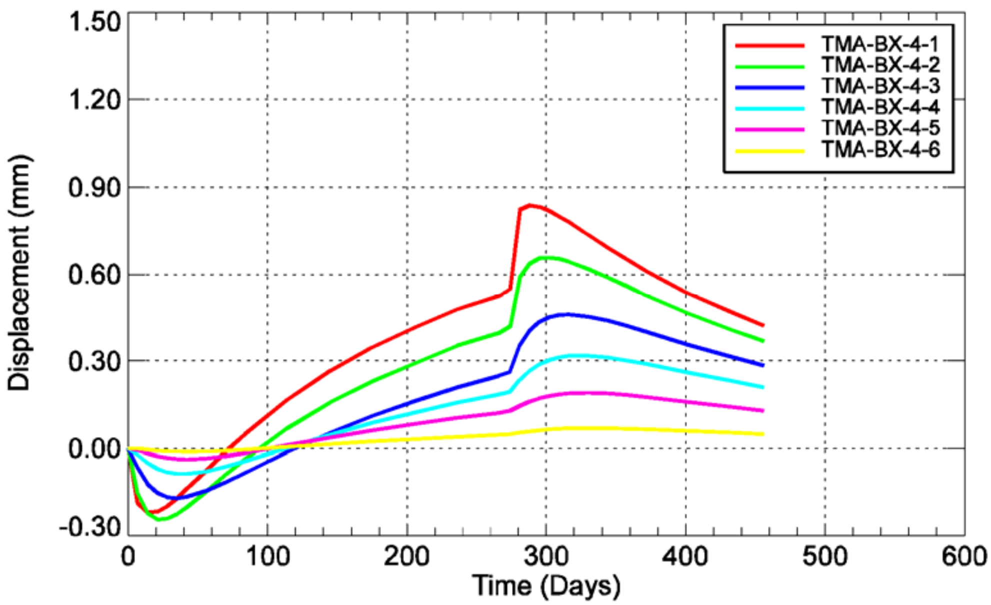

(b)

Figure 14. Measured (a) and pre-test predicted (b) displacement for six anchors along one subhorizontal extensometer borehole oriented normal to the heat sources [Cho, 1999].

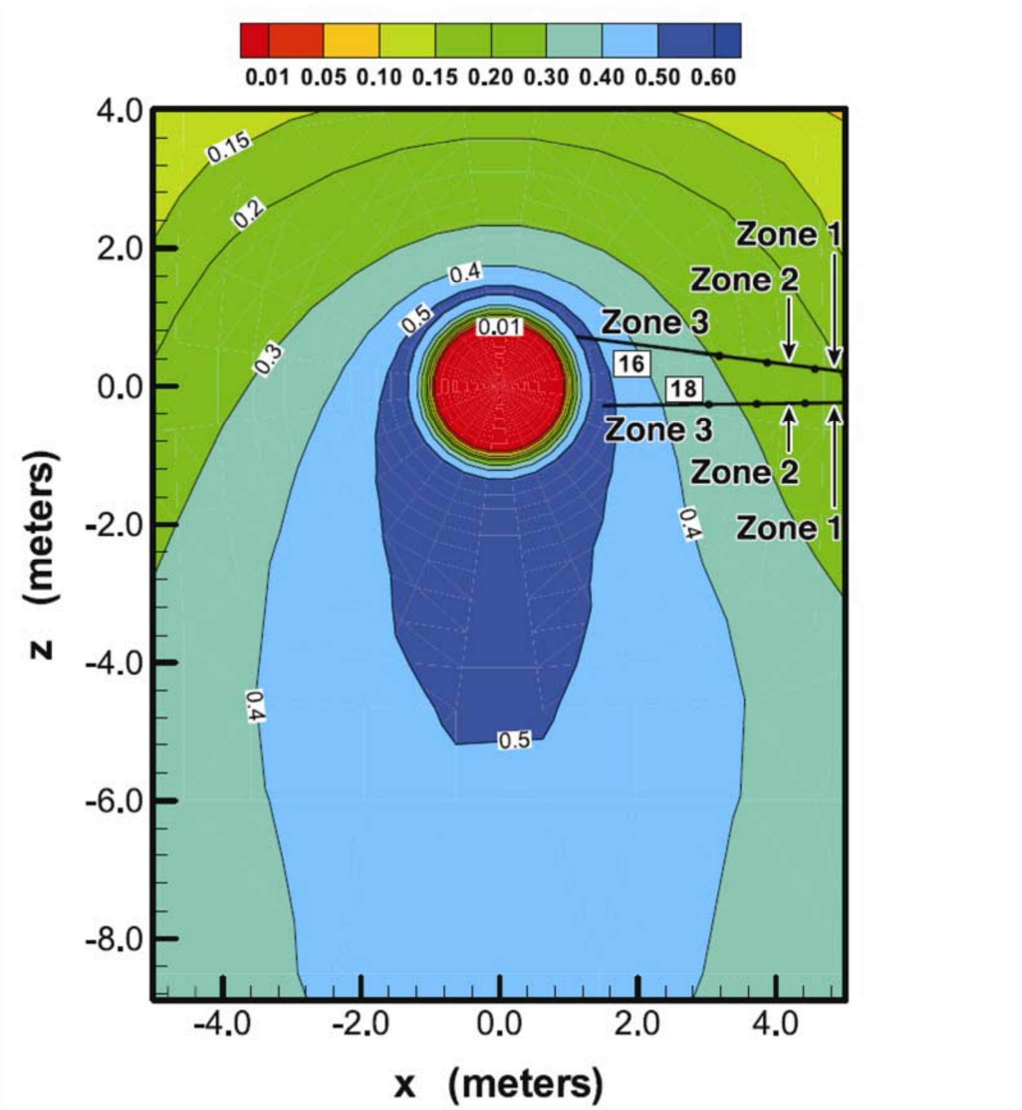

Figure 15. Simulated fracture liquid saturation at 9 months of heating in single-heater test vertical cross section intersecting the in the middle of the heater [Tsang et al., 2009].

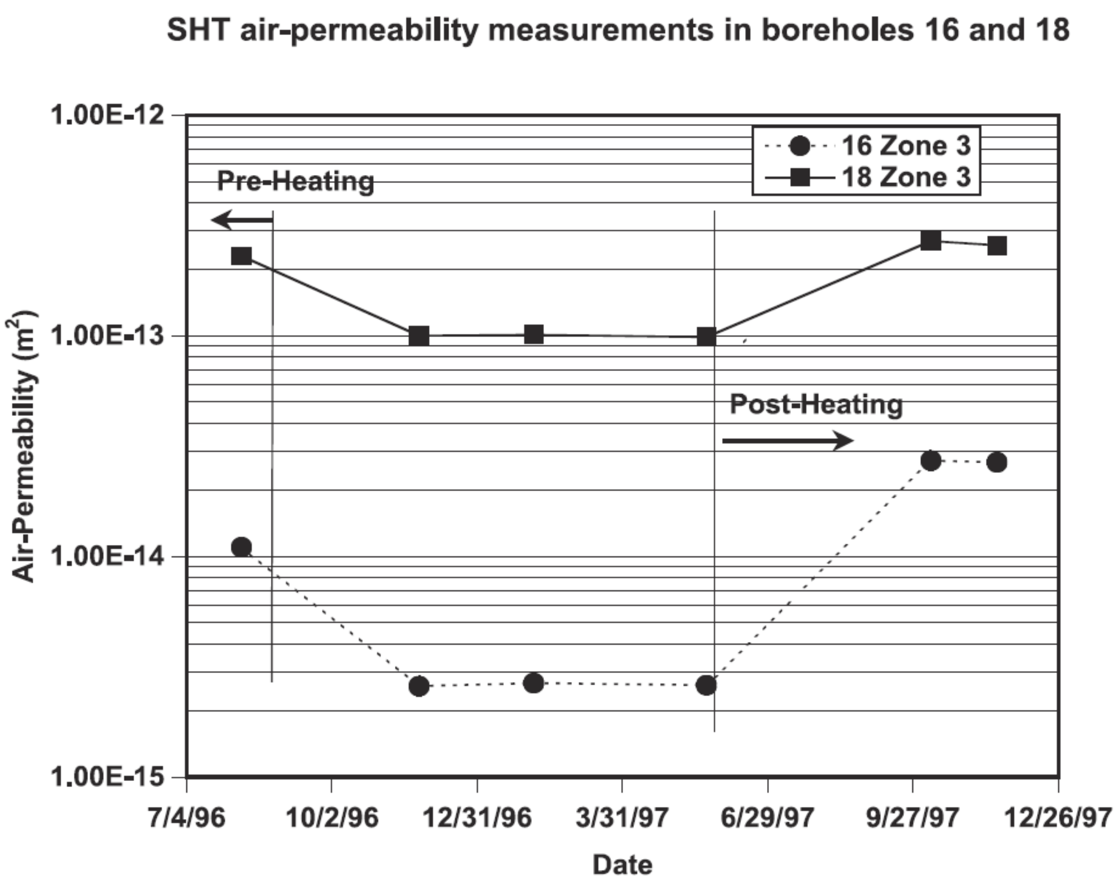

Figure 16. Evolution of air permeability measurements measured in packed off borehole sections at various distances from the heat source before, during and after heating phase of the SHT [Tsang et al., 2009].

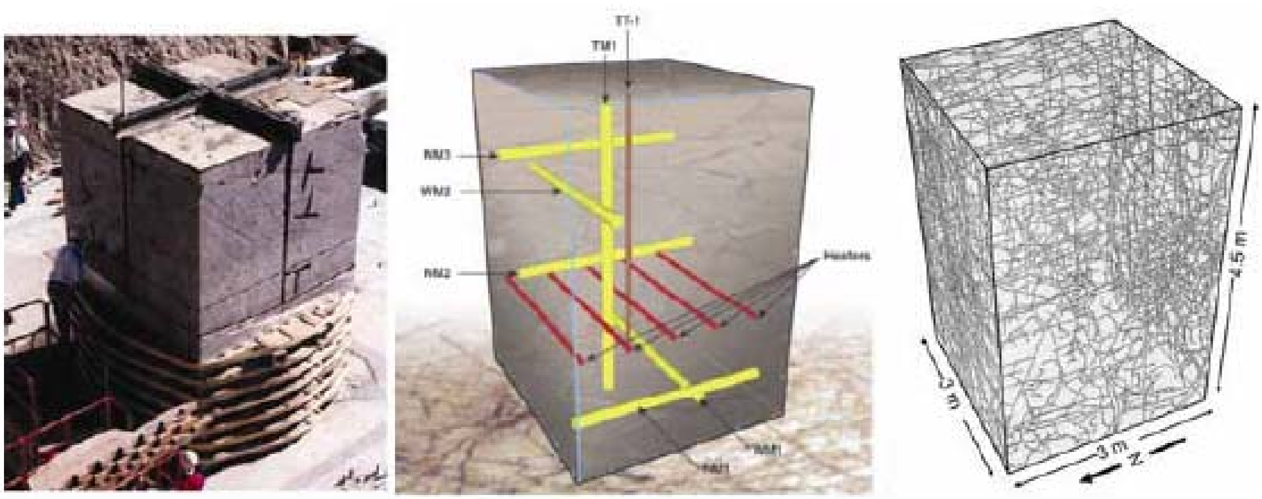

Figure 17. (a) Photo of the LBT block of Topopah Spring Tuff at Fran Ridge, (b) Schematic three-dimensional perspective of the LBT showing heaters and boreholes for monitoring of displacements [Blair, 2001] and (c) mapped fractures [Lin et al. 2001].

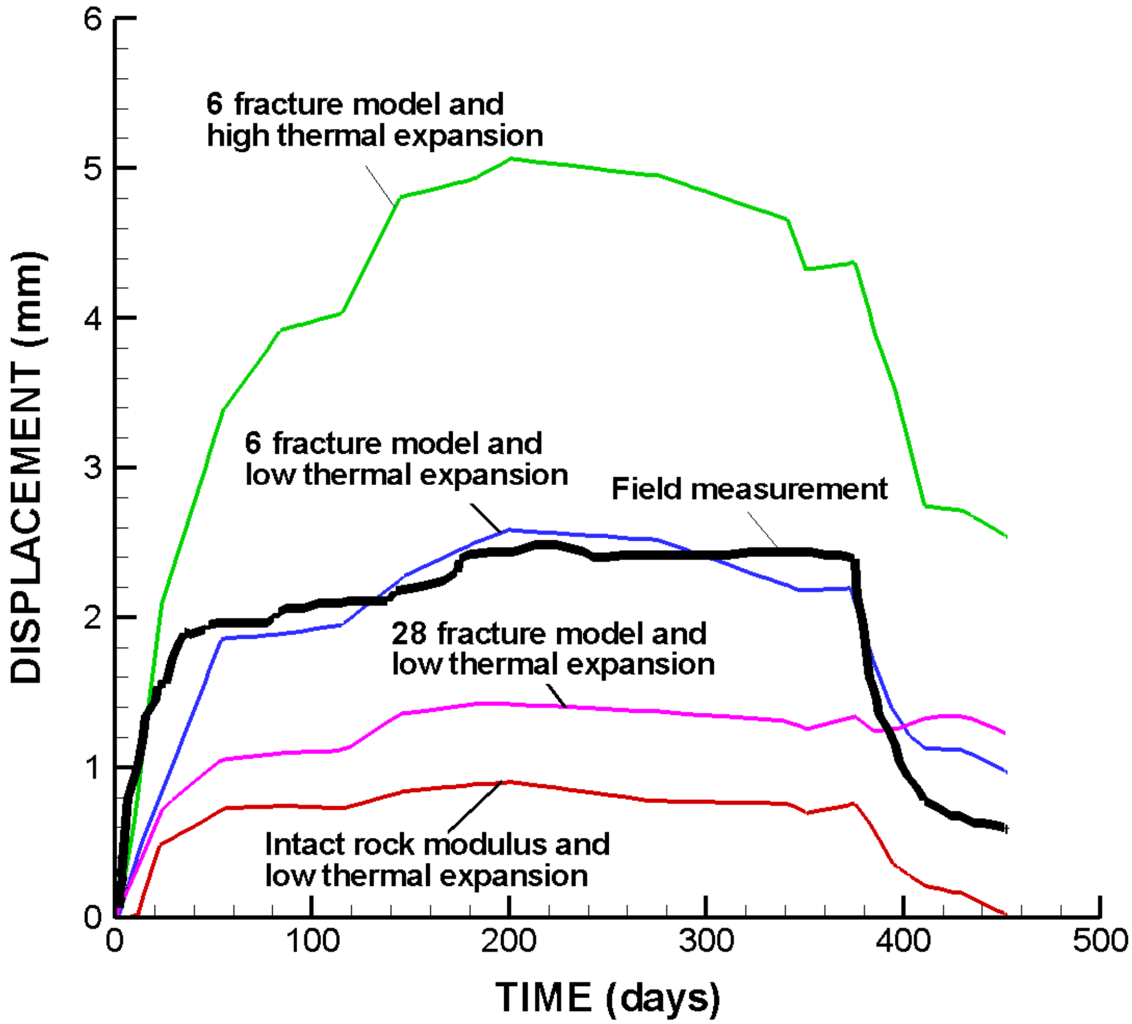

Figure 18. Modeling results for relative displacement along WM2 (modified from Blair [2001]).

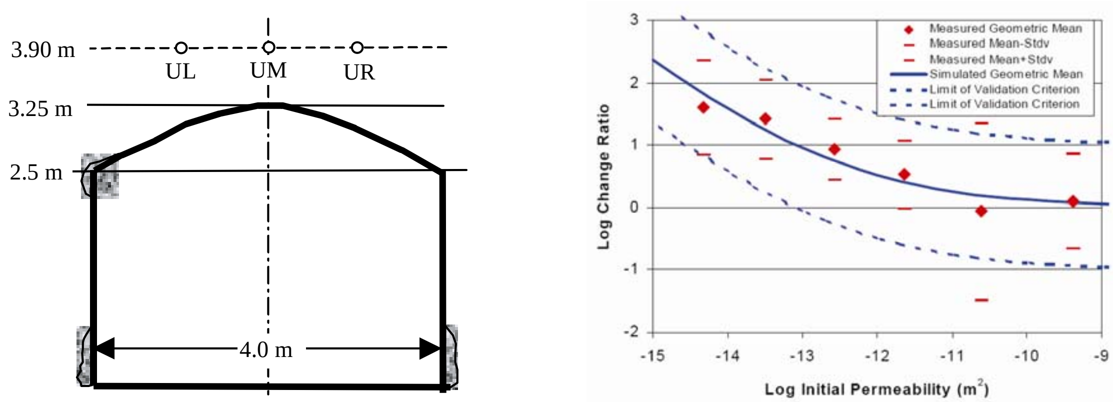

Figure 19. Pre/post-excavation permeability tests conducted in partially saturated tuff at Yucca Mountain. (a) Geometry of the tunnel and test boreholes, and (b) measured and simulated ratio of pre- and post-excavation permeability plotted against pre-excavation permeability [Rutqvist, 2004].

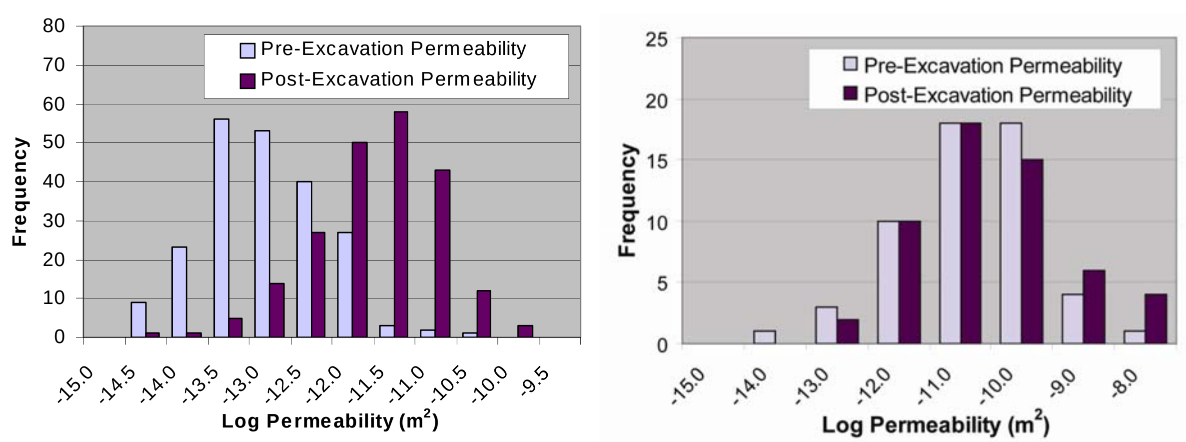

Figure 20. Histogram of permeability distribution derived from permeability measurements before and after excavation for (a) four niches excavated in the Tptpmn unit, and for (b) one niche excavated in the Tptpll unit [Rutqvist, 2004].

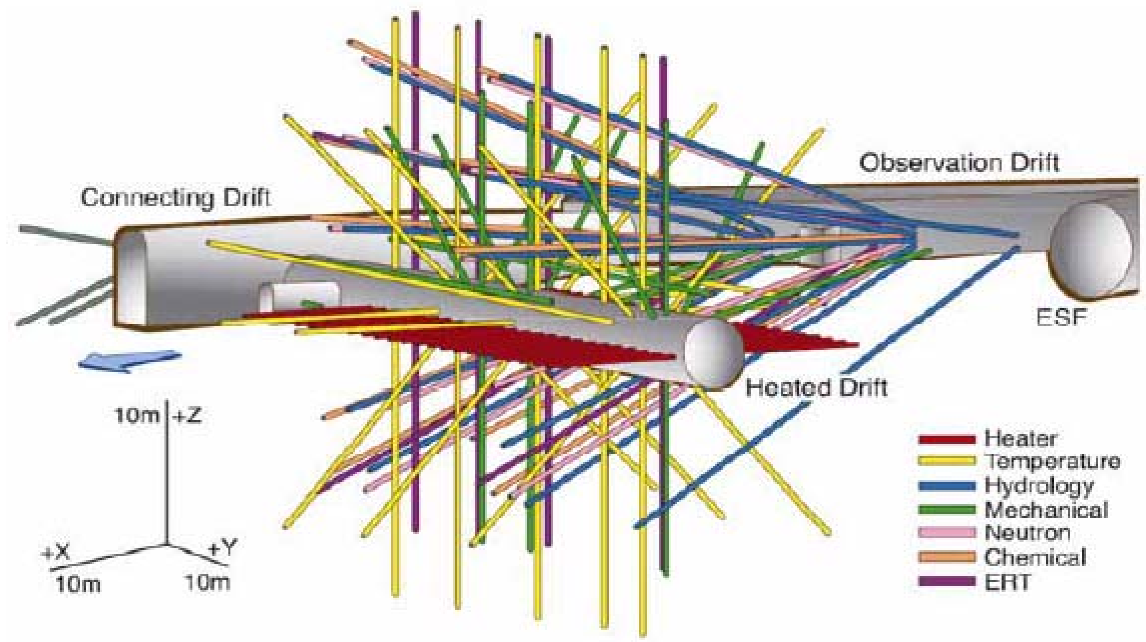

Figure 21. Three-dimensional view of the Yucca Mountain Drift Scale Test. The color-coded lines indicate boreholes for various measurements of thermally driven THMC responses [Tsang et al., 2009].

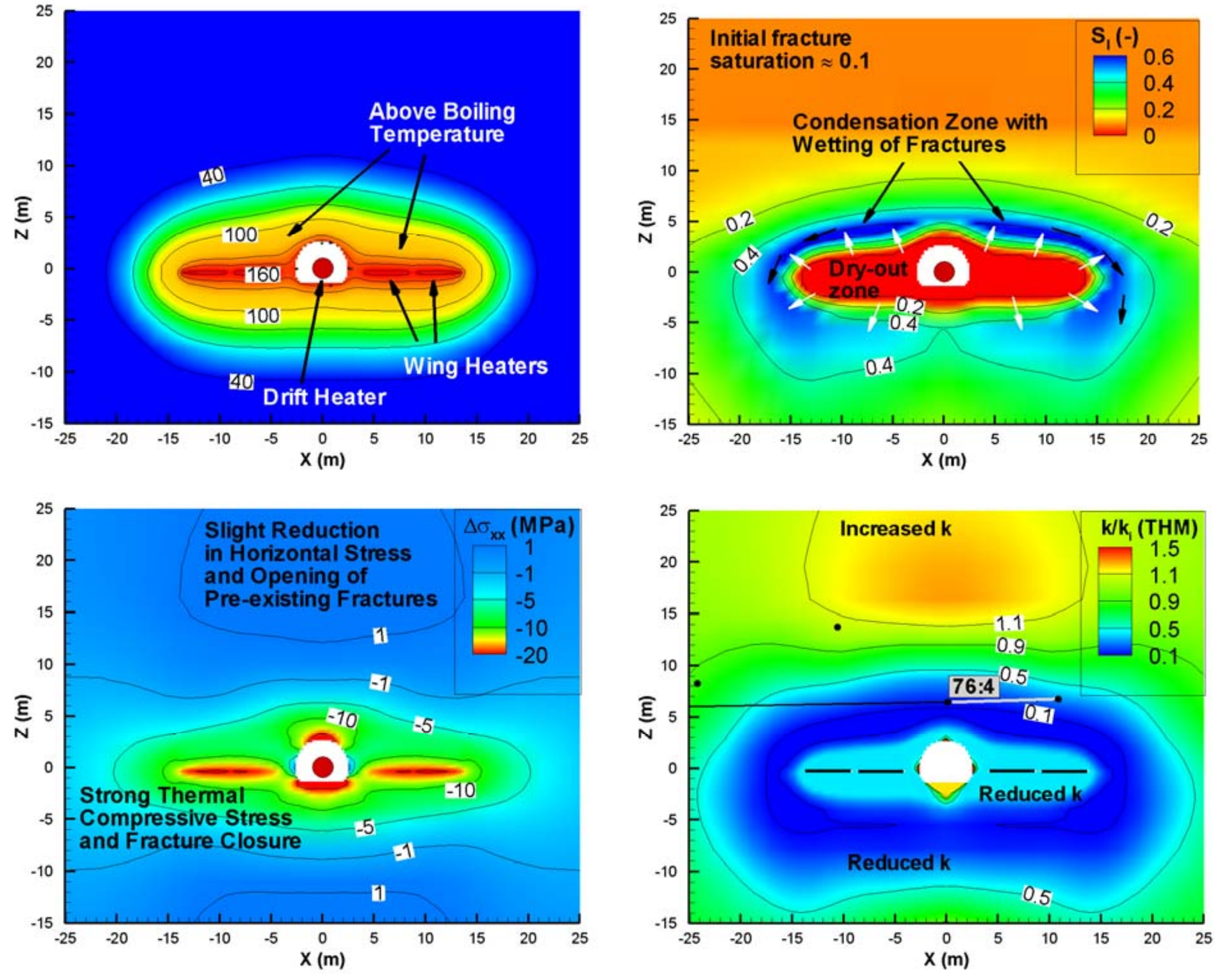

Figure 22. Calculated contours of (a) temperature, (b) change in liquid fracture saturation, (c) change in horizontal stress, and (d) permeability change factor in the NW-striking fracture set after 1 year of heating [Rutqvist et al. 2005].

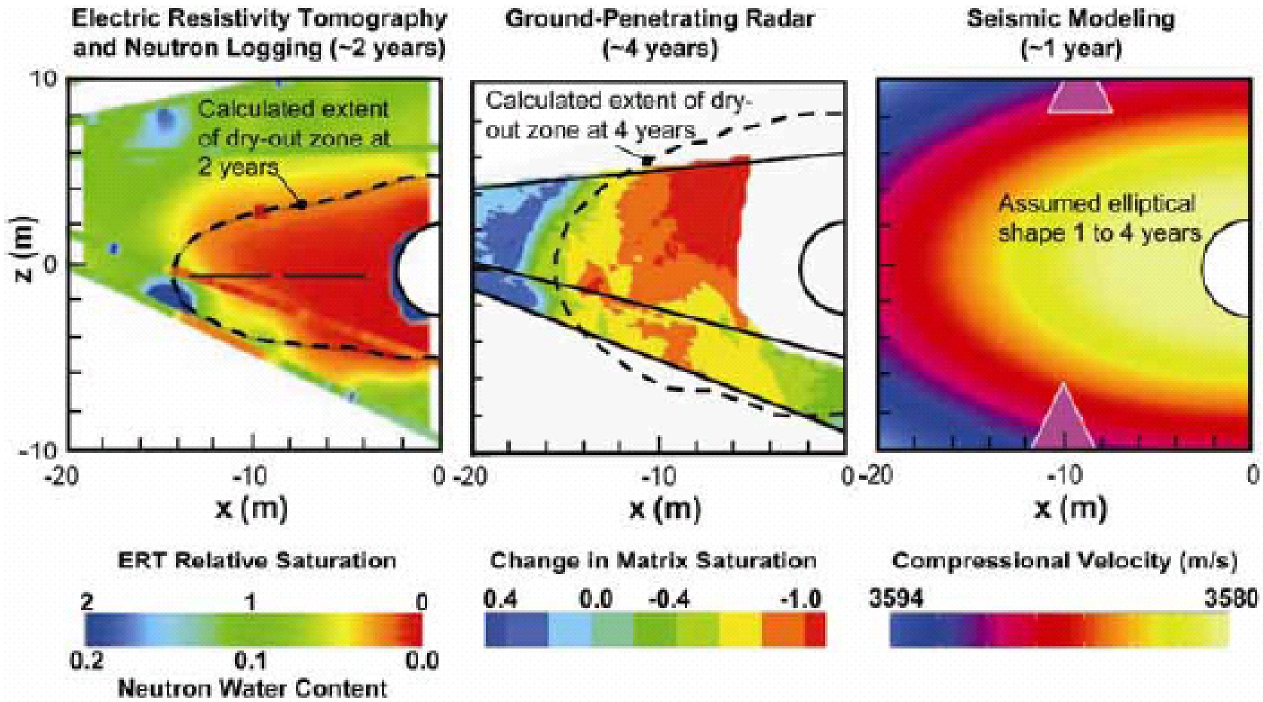

Figure 23. Results of geophysical field measurement to evaluate changes in the superheated zone. The contours of ERT relative saturation and neutron water content (left) and change is matrix saturation inferred from ground-penetrating radar (middle) was extracted from Tsang et al. [2009], whereas compressional velocity contour (right) was extracted from Smith and Snieder [2010]. Dashed lines in the left and middle figure are the calculated extent of the dryout zone corresponding to the extent of the <50% matrix saturation; Note that the seismic velocity change (right) was evaluated for an assumed elliptically shaped velocity structure that was also assumed to be constant over the 4 years of heating.

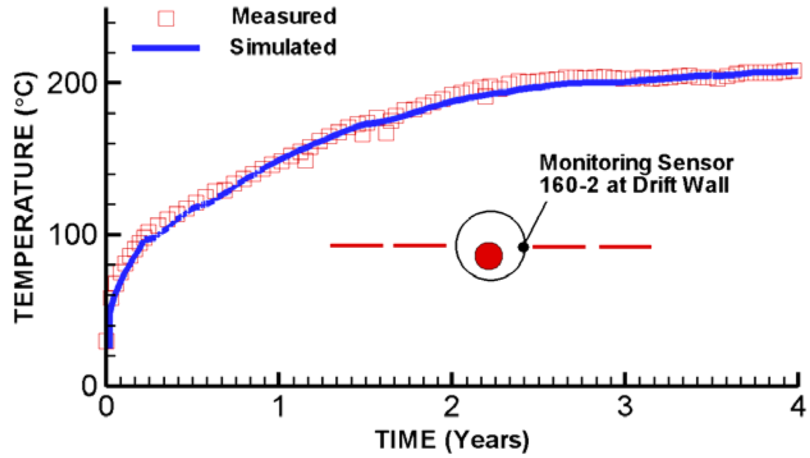

(a)

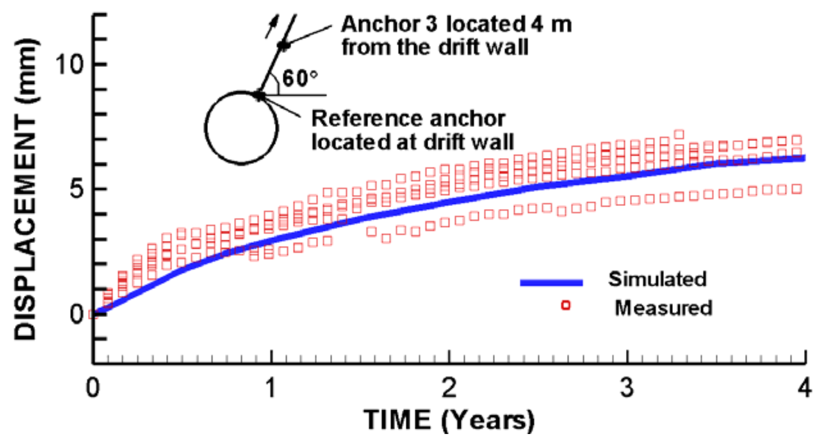

(b)

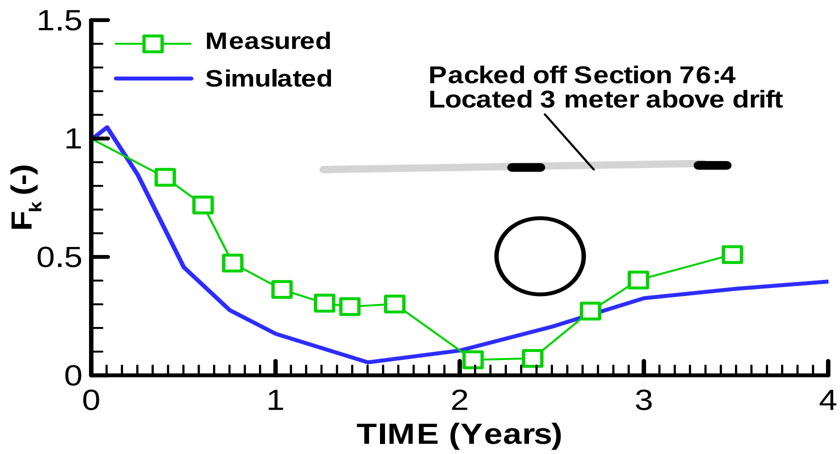

(c)

Figure 24. Comparison of simulated and measured temperature, displacement, and permeability change factor [Rutqvist, 2004].

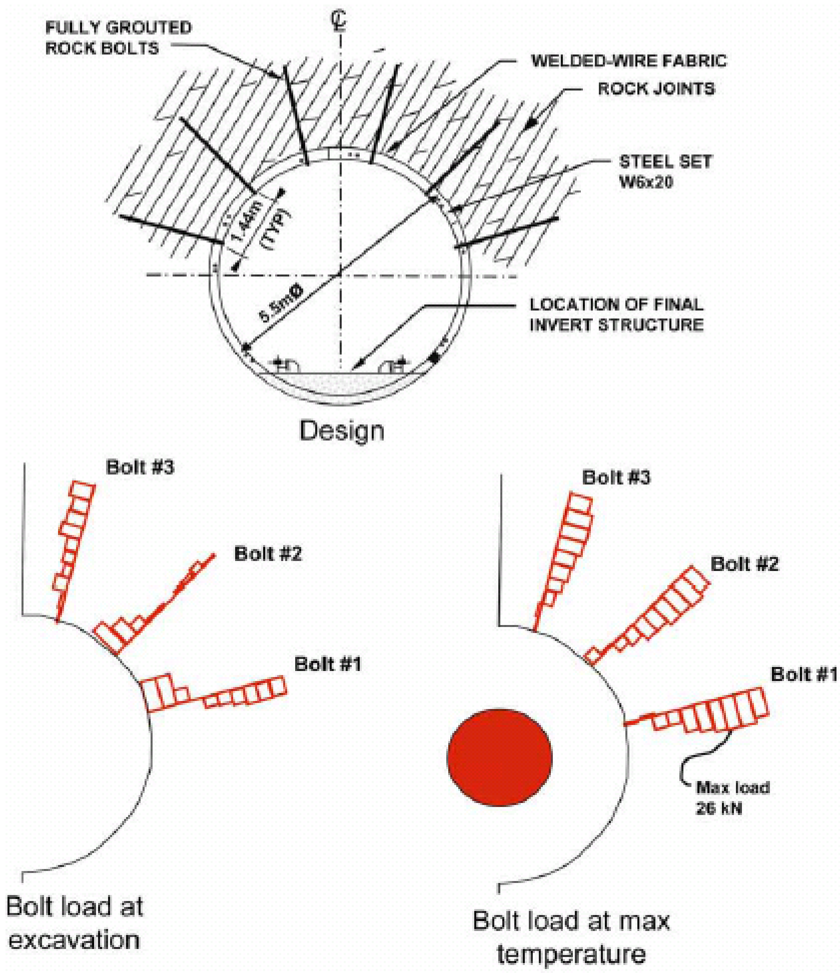

Figure 25. Ground support for emplacement drifts with steel sets and fully grouted rock bolts (top), and (bottom) calculated axial forces along rock bolts for in situ and thermal load (modified from Sun et al. [2001]).

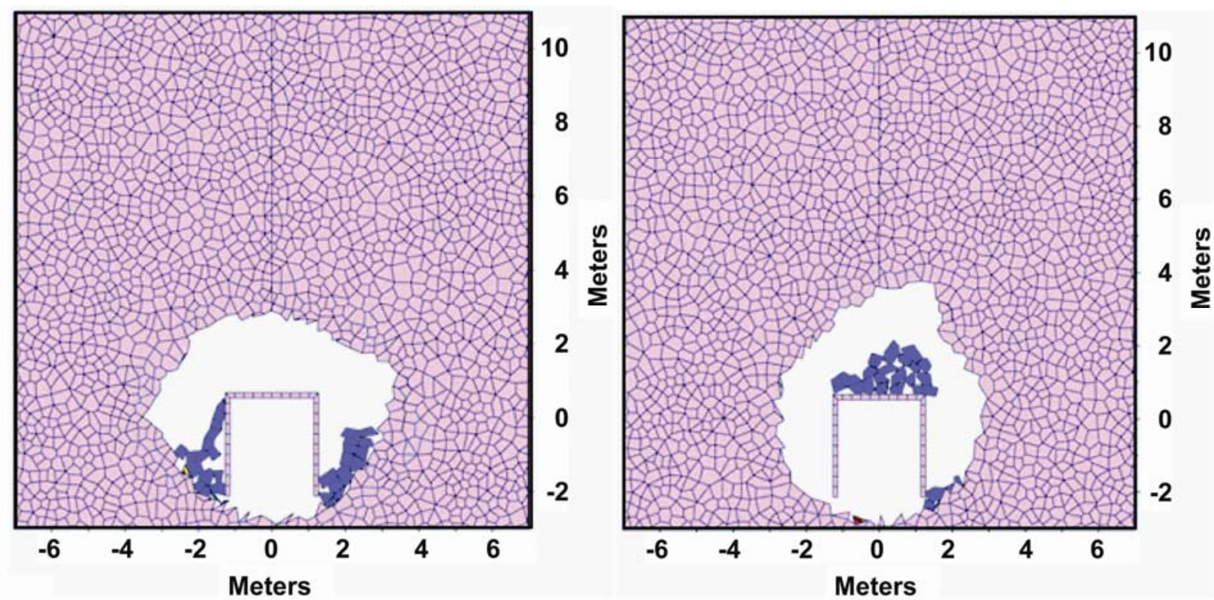

Figure 26. Calculated rock fall after 10,000 years caused by the combined effects of in situ stress, thermal stress, and time-dependent strength degradation for a drift located in (a) Category 2 and (b) Category 5, lithophysal rock [Kicker et al., 2004, Damjanac et al., 2007]

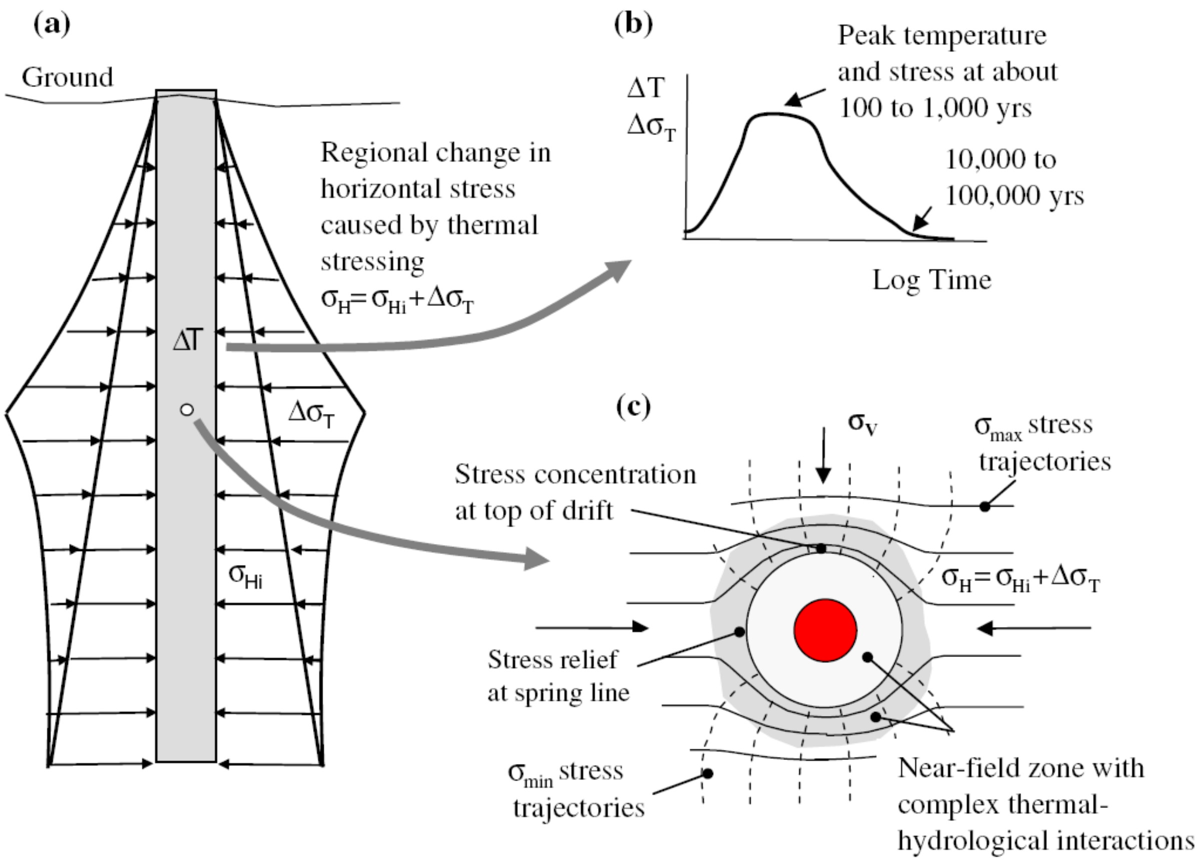

Figure 27. Schematic of thermally driven mechanical changes around a repository tunnel [Rutqvist et al., 2009].

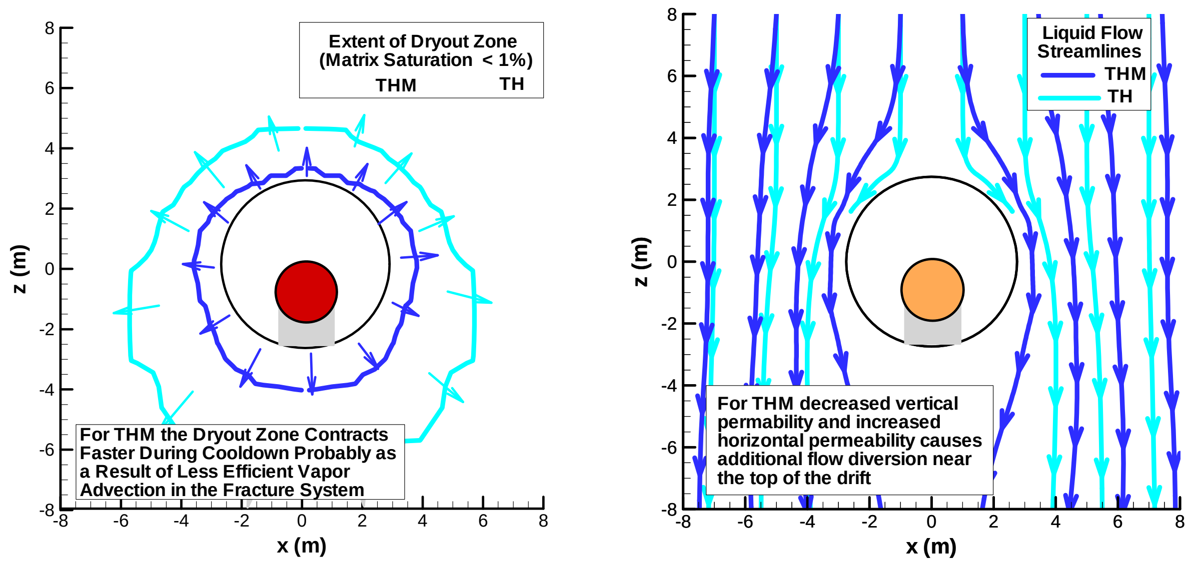

(a) (b)

Figure 28. Effects of THM-induced changes in hydrological properties. (a) Effects on the extent of the dryout zone after 1000 years, and (b) effects on the liquid fluid flow pattern at 10,000 years [Rutqvist et al., 2009].